

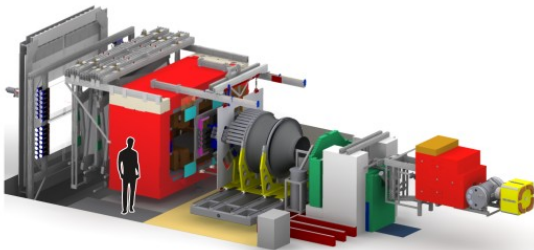
RECENT RESULTS FROM BGOOD

Rachele Di Salvo



Roma "Tor Vergata"

- **Photoproduction off nucleons and physics motivations**
- **The BGOOD Detector**
- **Overview of analysis and results**



R. Di Salvo - NSTAR22 - Oct. 20th, 2022



BARYON RESONANCES AND MESON PHOTOPRODUCTION OFF NUCLEONS

Physics motivation for the study of photon-induced meson production off nucleons is the investigation of the **excitation spectrum of the nucleon**.

→ Static and dynamical properties of baryon resonances are the testing ground for our “understanding” of the quark structure of the matter.

Baryon resonances have been first observed in πN scattering and most states listed in PDG and their properties have been extracted from πN data.

BUT

in the last 30 years large efforts have been done to perform experiments with real and virtual photons at high duty-cycle facilities and dedicated apparatus for detection.

Particle	J^P	Year	Overall status		
				$N\gamma$	$N\pi$
N(1860)	$5/2^+$	1996	-	-	-
		2018	**	*	**
N(1875)	$3/2^-$	1996	-	-	-
		2018	***	**	**
N(1880)	$1/2^+$	1996	-	-	-
		2018	***	**	*
N(1895)	$1/2^-$	1996	-	-	-
		2018	****	****	*
N(1900)	$3/2^+$	1996	**		**
		2018	****	****	**

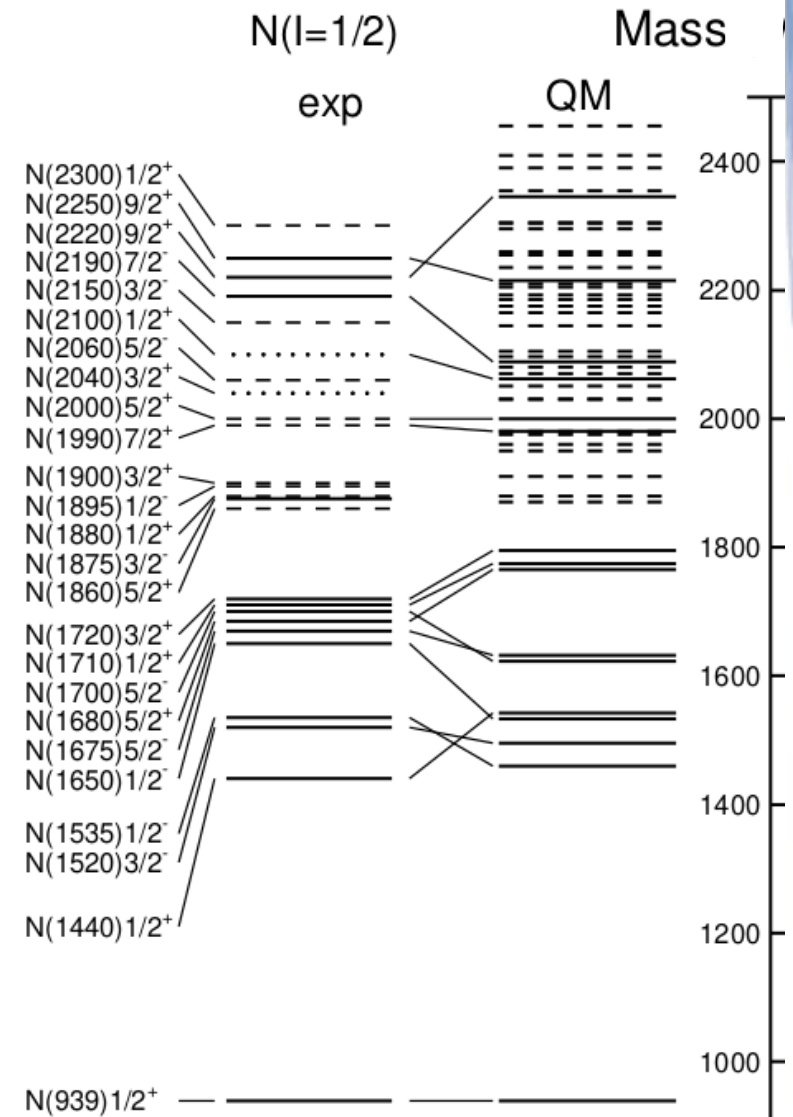
BARYON RESONANCES AND MESON PHOTOPRODUCTION OFF NUCLEONS

OPEN PROBLEMS

➡ “MISSING RESONANCES”

→ effective degrees of freedom inside the nucleon

➡ NATURE OF CERTAIN RESONANCES (not well explained by conventional models) → meson-baryon molecular states

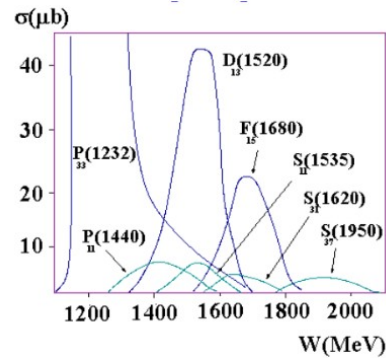


R. Di Salvo - NSTAR22 - Oct. 2

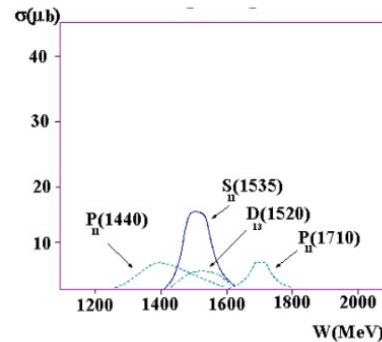
Meson photoproduction allows:

- + access to resonance states coupled to photons → ACCESS TO FINAL STATES DIFFERENT FROM πN → “MISSING RESONANCES”?
 - + polarization observables are accessible → SEPARATION OF OVERLAPPING RESONANCES
 - + decay amplitudes extraction → STUDY OF RESONANCE NATURE
 - low e.m. cross-sections → Overcome thanks to technological developments
 - non-resonant contributions are significant → Disentagled with polarization observables
- N.B. isospin filters (η , η' , ω) → ACCESS TO N^* RESONANCES

$\gamma p \rightarrow \pi^0 p$

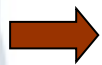


$\gamma p \rightarrow \eta p$



From B.Krusche, *Prog. Part. Nucl. Phys.* 51 (2003), 399-485

N.B. Photoproduction amplitudes on **proton** and **neutron** of the same meson (in its different charge states) can be decomposed in terms of isospin amplitudes.



NEED FOR EXPERIMENTS ON NEUTRONS AND PROTONS

AN EXAMPLE: THE η PHOTOPRODUCTION

Let us see the expressions for unpolarized cross section and beam asymmetry in terms of multipoles for η photoproduction case, obtained after truncation at the first orders:

$$\left(\frac{d\sigma}{d\Omega}\right)_{\text{UNP}} = \frac{q^{\text{CM}}}{2 k_{\text{Y}}^{\text{CM}}} \left(|E_{0+}|^2 \right) \text{Re} \left[E_{0+}^* (E_{2-} - 3M_{2-}) \right] +$$

$$+ 2 \cos \theta \text{Re} \left[E_{0+}^* (3E_{1+} + M_{1+} - M_{1-}) \right] + 3 \cos^2 \theta \text{Re} \left[E_{0+}^* (E_{2-} - 3M_{2-}) \right]$$

$$\Sigma = - \frac{q^{\text{CM}}}{2 k_{\text{Y}}^{\text{CM}}} \frac{1}{\left(\frac{d\sigma}{d\Omega}\right)_{\text{UNP}}} 3 \sin^2 \theta \text{Re} \left[E_{0+}^* (E_{2-} + M_{2-}) \right]$$

$$\begin{aligned} E_{0+} &\rightarrow S_{11} \\ M_{1-} &\rightarrow P_{11} \\ E_{1+}, M_{1+} &\rightarrow P_{13} \\ E_{2-}, M_{2-} &\rightarrow D_{13} \end{aligned}$$

Further term is: $(g \sin^2 \theta \cos \theta)$
(interference S_{11} - F_{51})

Since the E_{0+} multipole dominates at threshold, in the differential cross-section it is hard to distinguish the contribution of other resonances.

In beam asymmetry, on the contrary, this contribution is amplified in the interference with the dominating multipole E_{0+} .



NEED FOR POLARIZED BEAMS AND/OR TARGETS EXPERIMENTS

STRANGENESS PHOTOPRODUCTION

In the last years focus has been put on the investigation of unconventional multi-quark states.

Interest has been fueled by discoveries, in the (hidden) charm sector, of:

X(3872) @ BELLE (PRL91, 262001, 2003)

X(3872) @ Babar (PRD77 091101, 2008)

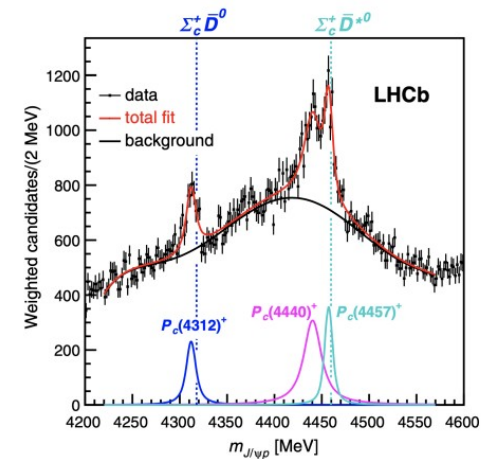
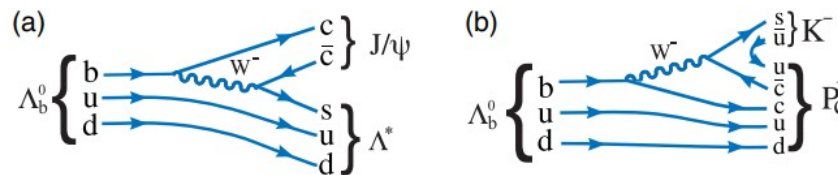
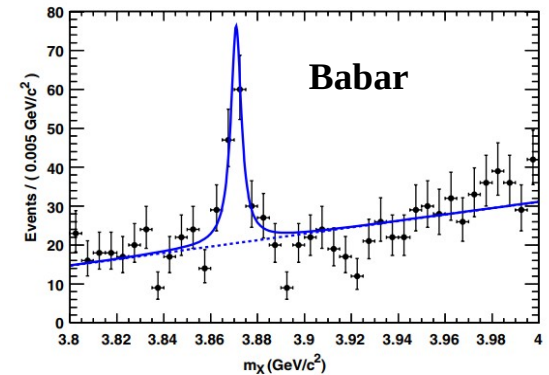
$B^+ \rightarrow K^+ \pi^+ \pi^- J/\psi$ very close to $D^0 \bar{D}^{*0}$ threshold
interpreted as a tetraquark state

P_c (4380/4450) states @ LHCb (PRL 115, 072001, 2015)

observed in $M(J/\psi p)$ distributions

predicted in **Wu et al., PRL 105, 232001 (2010)**

interpreted as pentaquark states



Parallels between the charm and strange sectors are possible and predictions for lighter multi-quark states can be done (exchanging a $c \rightarrow s$), that can be interpreted as meson-baryon molecular-type structures.

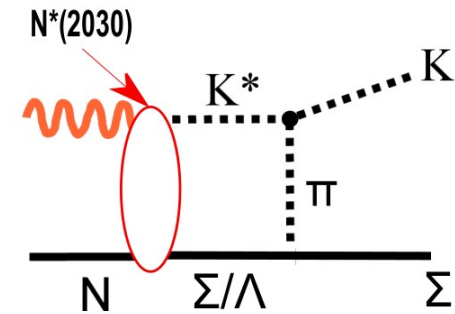
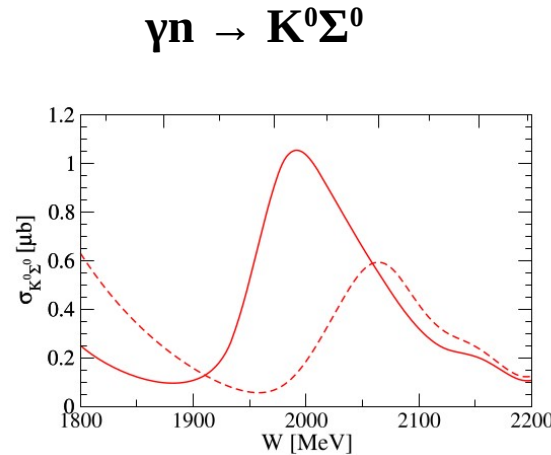
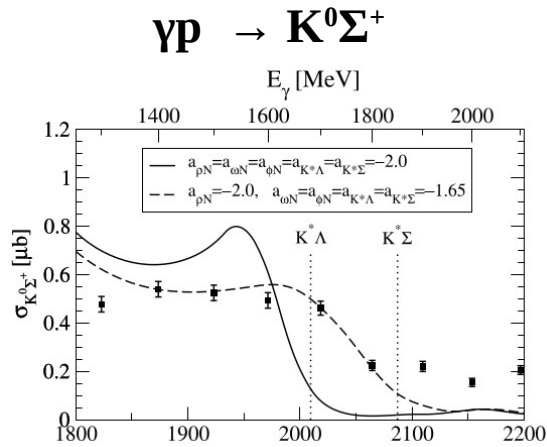
- See **Katrin Kohl's talk** (Oct. 18th @ 15:00)
- See **Johannes Groß' talk** (Oct 19th @ 15:40)

The same model that predicts P_C states (A. Ramos and E. Oset, Phys. Lett. B 727, (2013) 287):

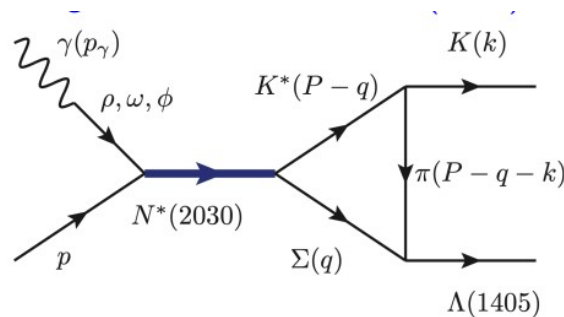
- explains the cusp observed in $K^0\Sigma^+$ (CBELSA/TAPS Phys. Lett. B 713 (2012) 180)

- predicts an enhancement in $K^0\Sigma^0$ on the neutron

due to destructive/constructive interference between $K^*\Lambda$ and $K^*\Sigma$ states magnified by a same resonance $N^*(2030)$, a loosely bound $K^*\Sigma$ state.



Same resonance $N^*(2030)$ could be responsible for $\Lambda(1405)$ photoproduction via the triangle singularity (E. Wang, et al., Phys. Rev. C 95 (2017) 015205)



BGOballOpenDipole magnet Collaboration

- ⇒ A collaboration has been established in 2009 (~ 50 collaborators, **Germany, Italy, Great Britain, Russia, Switzerland, Ukraine**)
- **LoI** signed and accepted at the PAC Mainz-Bonn 2009, June 25th-26th
- **MoU** signed on 2010, March 9th

Location:

S-Beamline

ELSA Accelerator in Bonn

Beam:

polarized and tagged photon beam in the energy range 0.2-3. GeV

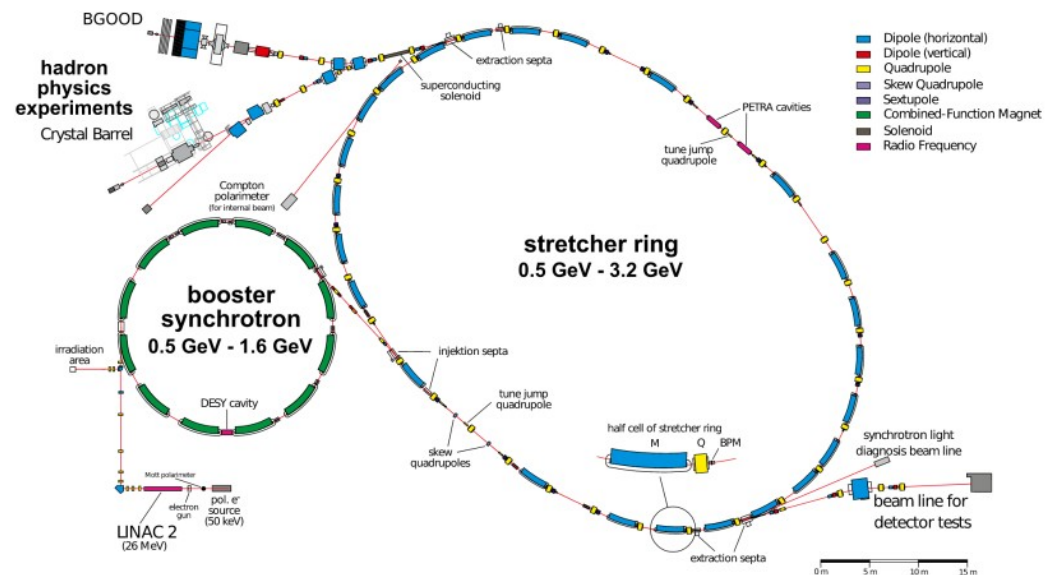
Spokespersons:

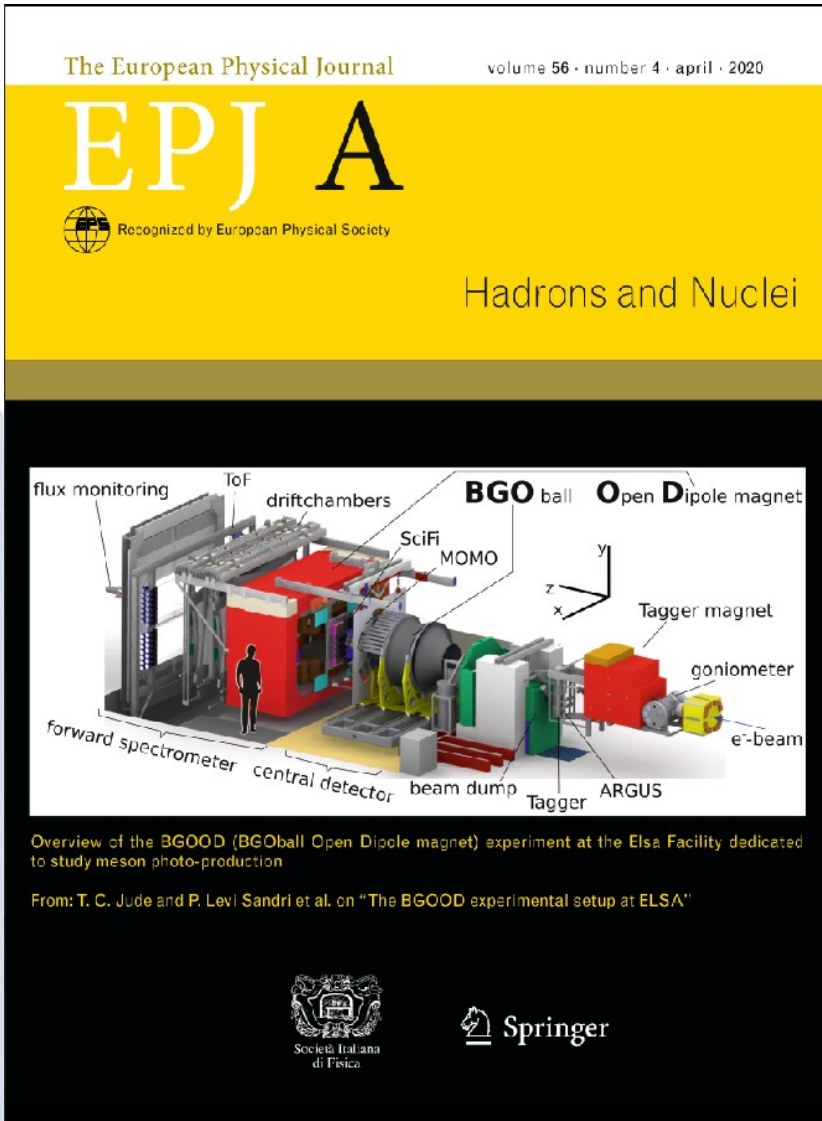
H. Schmieden, P. Levi Sandri

Italian Responsible:

P. Levi Sandri (2015 → today)

R. Di Salvo (2008 → 2015)





Eur. Phys. J. A (2020) 56:104
<https://doi.org/10.1140/epja/s10050-020-00107-x>

THE EUROPEAN
 PHYSICAL JOURNAL A



Regular Article - Experimental Physics

The BGOOD experimental setup at ELSA

S. Alef¹, P. Bauer¹, D. Bayadilov^{2,3}, R. Beck², M. Becker², A. Bella¹, J. Bieling², S. Böse², A. Braghieri⁴, K.-Th. Brinkmann⁵, P. L. Cole⁶, R. Di Salvo⁷, D. Elsner¹, A. Fantini^{7,8}, O. Freyermuth¹, F. Frommberger¹, G. Gervino^{9,10}, F. Ghio^{11,12}, S. Goertz¹, A. Gridnev³, E. Gutz⁵, D. Hammann¹, J. Hannappel^{1,19}, W. Hillert^{1,19}, O. Jahn¹, R. Jahn², J. R. Johnstone¹, R. Joosten², T. C. Jude^{1,a}, H. Kalinowsky², V. Kleber^{1,20}, F. Klein¹, K. Kohl¹, K. Koop², N. Kozlenko³, B. Krusche¹³, A. Lapik¹⁴, P. Levi Sandri^{15,b}, V. Lisin¹⁴, I. Lopatin³, G. Mandaglio^{16,17}, M. Manganaro^{16,17,21}, F. Messi^{1,22}, R. Messi^{7,8}, D. Moriccianni⁷, A. Mushkarenkov¹⁴, V. Nedorezov¹⁴, D. Novinskiy³, P. Pedroni⁴, A. Polonskiy¹⁴, B.-E. Reitz¹, M. Romaniuk^{7,18}, T. Rostomyan¹³, G. Scheluchin¹, H. Schmieden¹, A. Stugelev³, V. Sumachev³, V. Tarakanov³, V. Vegna¹, D. Walther², H.-G. Zaunick^{2,5}, T. Zimmermann¹

¹ Rheinische Friedrich-Wilhelms-Universität Bonn, Physikalisches Institut, Nußallee 12, 53115 Bonn, Germany

² Rheinische Friedrich-Wilhelms-Universität Bonn, Helmholtz-Institut für Strahlen- und Kernphysik, Nußallee 14-16, 53115 Bonn, Germany

³ Petersburg Nuclear Physics Institute, Gatchina, Leningrad District 188300, Russia

⁴ INFN sezione di Pavia, Via Agostino Bassi, 6, 27100 Pavia, Italy

⁵ Justus-Liebig-Universität Gießen, II. Physikalisches Institut, Heinrich-Buff-Ring 16, 35392 Gießen, Germany

⁶ Department of Physics, Lamar University, Beaumont, TX 77710, USA

⁷ INFN Roma "Tor Vergata", Via della Ricerca Scientifica 1, 00133 Rome, Italy

⁸ Dipartimento di Fisica, Università di Roma "Tor Vergata", Via della Ricerca Scientifica 1, 00133 Rome, Italy

⁹ INFN sezione di Torino, Via P.Giuria 1, 10125 Turin, Italy

¹⁰ Dipartimento di Fisica, Università di Torino, via P. Giuria 1, 10125 Turin, Italy

¹¹ INFN sezione di Roma La Sapienza, P.le Aldo Moro 2, 00185 Rome, Italy

¹² Istituto Superiore di Sanità, Viale Regina Elena 299, 00161 Rome, Italy

¹³ Institut für Physik, Klingelbergstrasse 82, 4056 Basel, Switzerland

¹⁴ Russian Academy of Sciences Institute for Nuclear Research, Prospekt 60-letiya Oktyabrya 7a, Moscow 117312, Russia

¹⁵ INFN - Laboratori Nazionali di Frascati, Via E. Fermi 54, 00044 Frascati, Italy

¹⁶ INFN sezione Catania, 95129 Catania, Italy

¹⁷ Dipartimento MIFT, Università degli Studi di Messina, Via F. S. D'Alcontres 31, 98166 Messina, Italy

¹⁸ Institute for Nuclear Research of NASU, 03028 Kiev, Ukraine

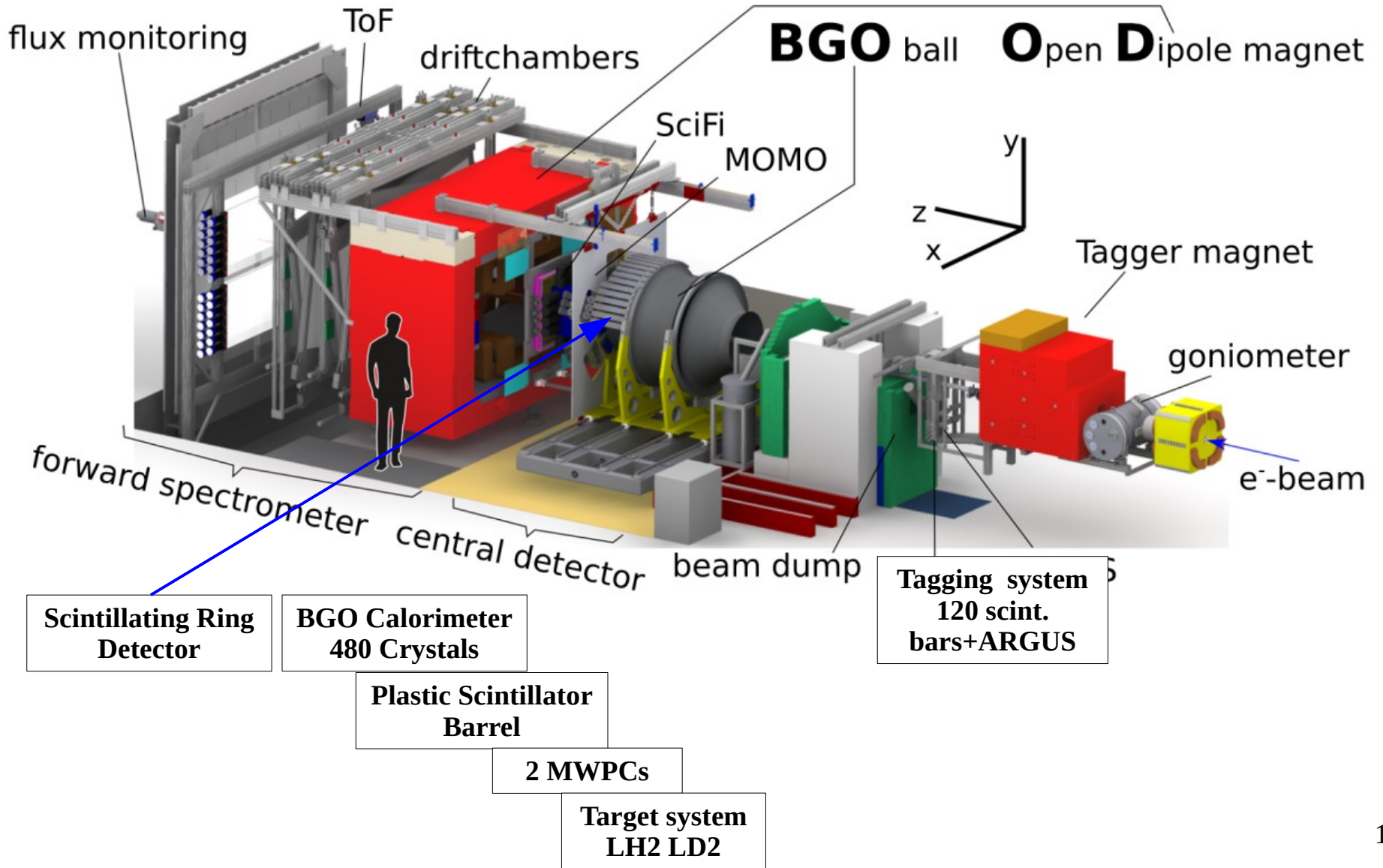
¹⁹ Present Address: DESY Research Centre, Hamburg, Germany

²⁰ Present Address: Forschungszentrum Jülich, Jülich, Germany

²¹ Present Address: University of Rijeka, Rijeka, Croatia

²² Present Address: Lund University & ESS, Lund, Sweden

BGOOD – The Detector



GENERAL FEATURES OF BGOOD

Setup is a **unique combination of:**

- **central region: large solid angle calorimeter with excellent energy resolution for photons and good detection efficiency for neutrons; charged particle tracking and identification; neutron/photon discrimination**

- **high momentum resolution forward tracking of charged particles**

and has trigger capabilities (trigger on the released energy in BGO)



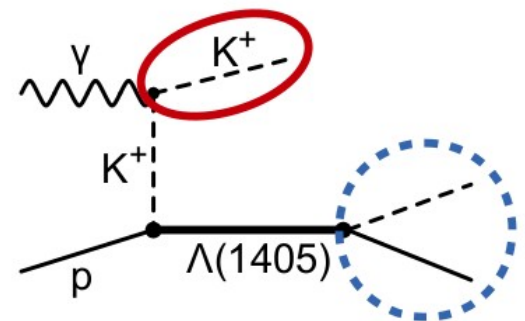
Ideally suited for:

- **mixed charged and neutral final state detection** (reconstruction of the complete kinematics of complex final states. both charged and neutrals)

- **investigation of kinematical regimes with minimal momentum transfer**

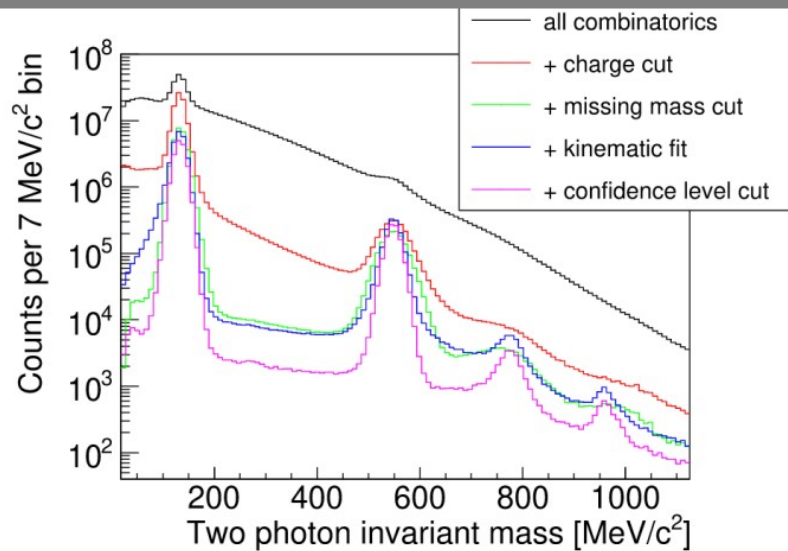
- **open trigger**

R. Di Salvo - NSTAR22 - Oct. 20th, 2022

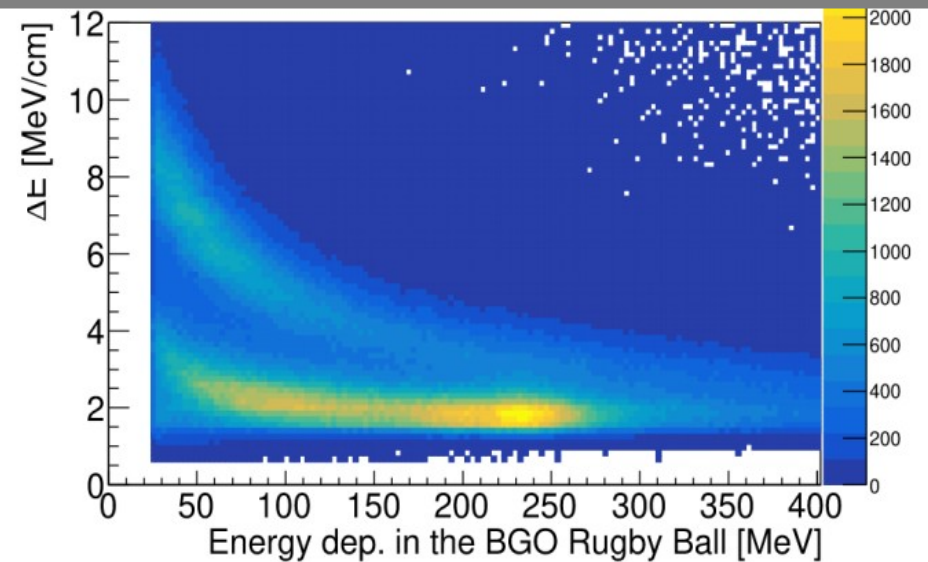


BGOOD Detector Performances

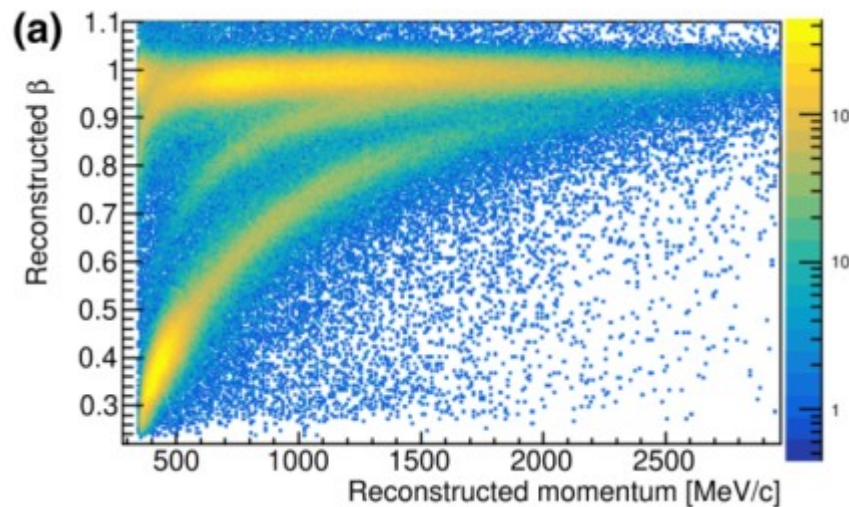
Photons in BGO Rugby Ball



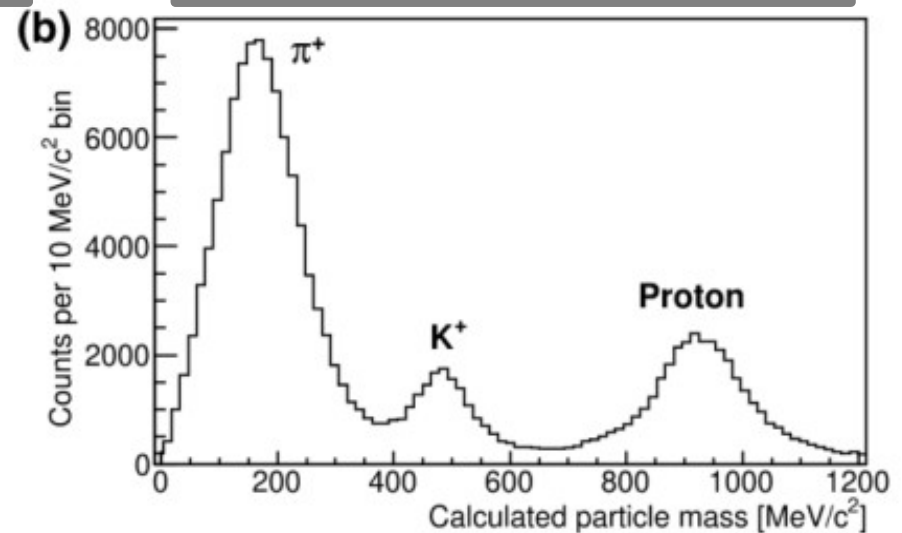
Pid BGORugbyBall-Plastic Scint. Barrel



β vs Momentum in Forw Spectr



Mass From ToF Walls



EXPERIMENTAL PROGRAM AT BGOOD

Extensive program for:

- strangeness photoproduction → CROSS SECTIONS

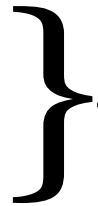
- $\gamma p \rightarrow K^+\Lambda$

- $\gamma p \rightarrow K^+\Sigma^0$



See Johannes Groß' talk (Oct 19th@ 15:40)

- $\gamma p \rightarrow K^+\Lambda(1405) \rightarrow K^+\pi^0\Sigma^0$



See Katrin Kohl's talk (Oct 18th@ 15:00)

- $\gamma n \rightarrow K^0\Sigma^0$

- $\gamma n \rightarrow K^+\Sigma^-$ (preliminary)



See Johannes Groß' talk (Oct 19th@ 15:40)

- baryon-baryon dynamics in the ud sector

- $\gamma d \rightarrow \pi^0\pi^0d$



See Tom Jude's talk (Oct 18th@ 15:40)

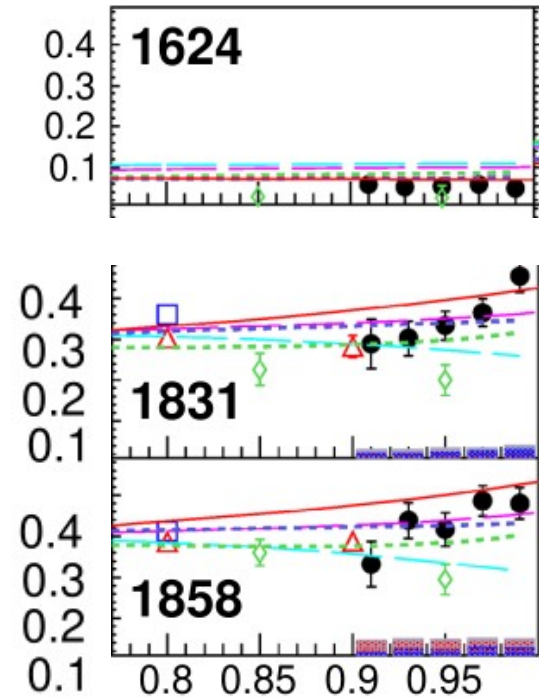
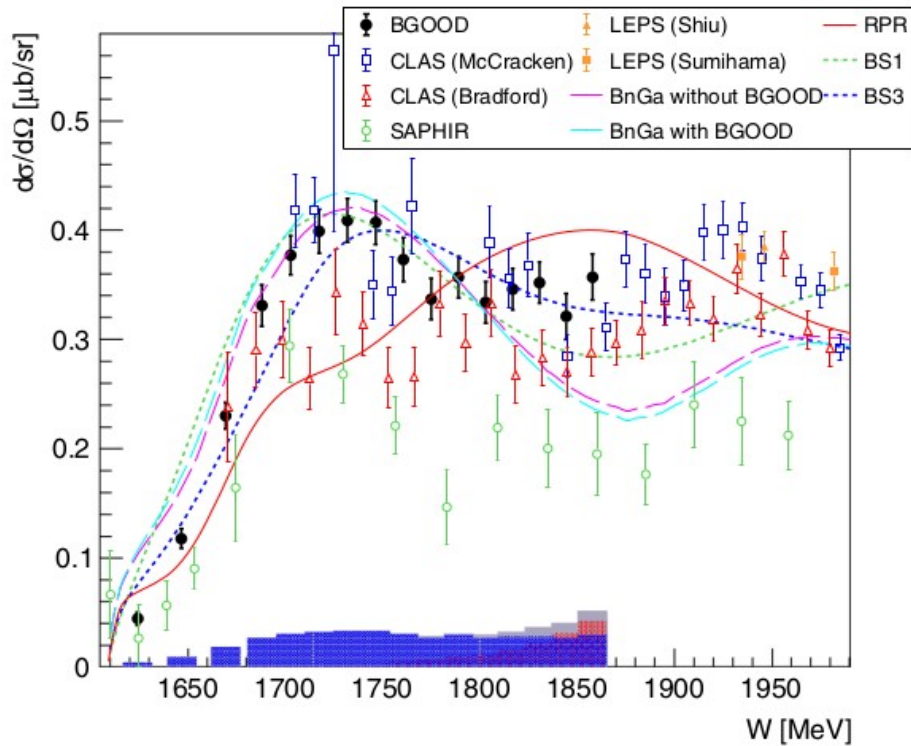
- pseudoscalar meson photoproduction → BEAM ASYMMETRIES

- $\gamma p \rightarrow \pi^0p$ $\gamma n \rightarrow \pi^0n$

- $\gamma p \rightarrow \eta p$ $\gamma n \rightarrow \eta n$

- $\gamma p \rightarrow \eta' p$

$\gamma p \rightarrow K^+ \Lambda$
 S. Alef *et al.*
 Eur. Phys. J. A (2021) 57:80



K^+ detected in forward spectrometer and $\Lambda \rightarrow \pi^0 n$ with 2γ in BGO

$$\cos\theta_{CM}^{K^+} > 0.9$$

- **VERY HIGH STATISTICS**

→ Diff x-section vs. $\cos\theta_{CM}$ in W bins is flat at threshold and more forward peaked for higher W , consisting with increasing t -channel K and K^* exchange processes.

- **VERY GOOD ANGULAR RESOLUTION IN THE FORWARD DIRECTION**

→ sensitivity to high spin states (3rd resonance region, only access to N^*)

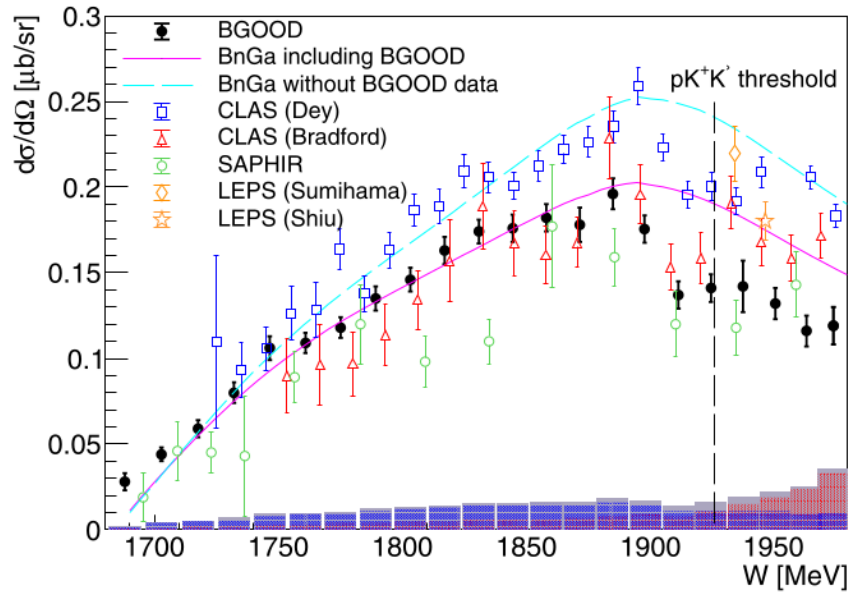
- **Structure visible at 1720 MeV** then data are more flat for energies above 1800 MeV.

Helpful in constraining elementary reaction mechanism for hypernuclei electroproduction¹⁴ at very low Q^2 , an important prerequisite to study hypernuclei.

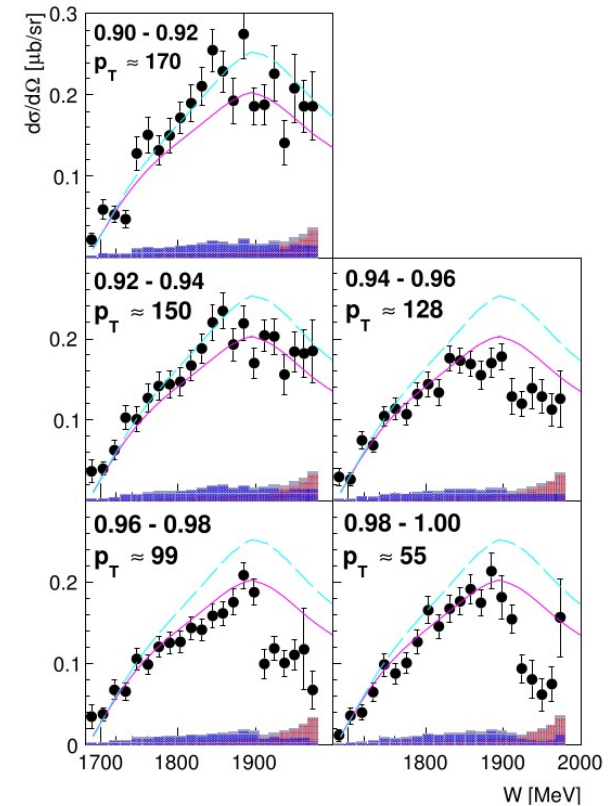
$\gamma p \rightarrow K^+ \Sigma^0$

T.C. Jude *et al.*

Phys. Lett. B 820 (2021), 136559



➔ See Johannes Groß' talk (Oct 19th@ 15:40)



K^+ detected in forward spectrometer and $\Sigma \rightarrow \Lambda \gamma$ with γ 's in BGO

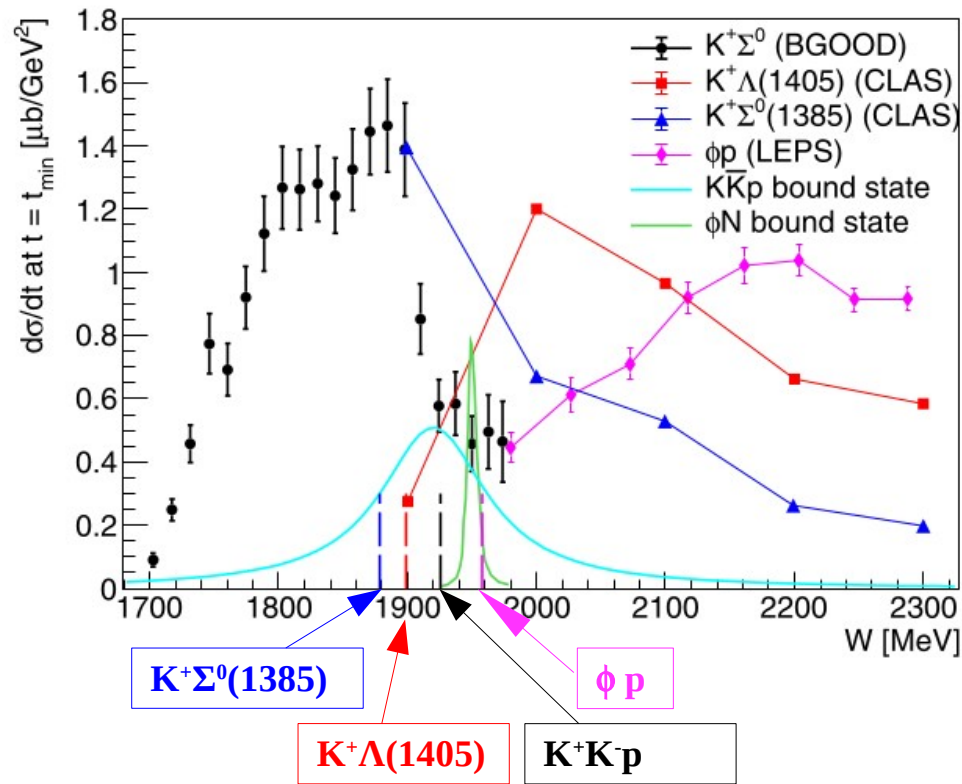
$$\cos\theta_{CM}^{K^+} > 0.9$$

• **VERY GOOD ANGULAR RESOLUTION IN THE FORWARD DIRECTION**

• **Cusp at $W=1900$ MeV where the x-sections drops by 1/3 over a 20 MeV range.**

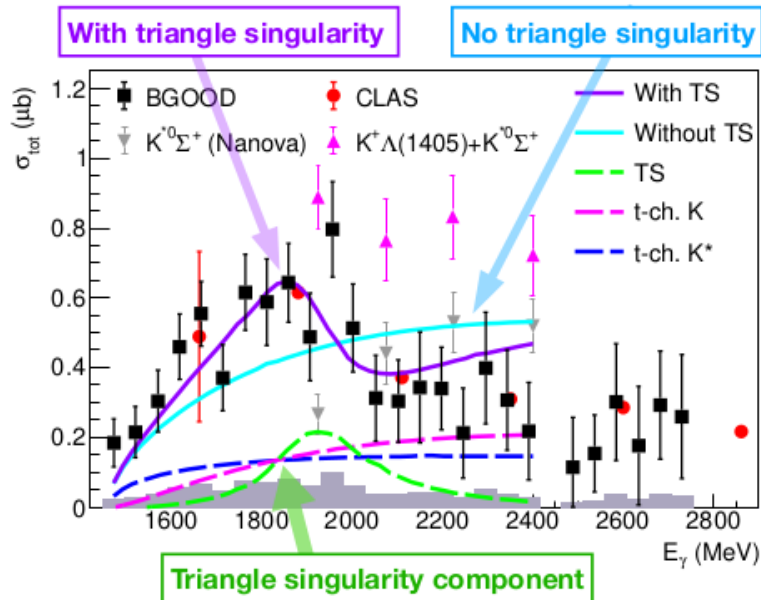
Structure nicely resolved in bins of θ_{CM} , (visible for $0.94 < \cos\theta_{CM} < 0.96$, pronounced for $\cos\theta > 0.98$).

• **ALMOST NO EXTRAPOLATION NEEDED TO $t=t_{min}$**



- In $d\sigma/dt$ drop very pronounced at $W=1900$ MeV.
- Drop due to pentaquark $X(2000)$? (proposed by the Sphinx Collaboration (for $p_T < 141$ MeV) in diffractive $p+C \rightarrow [K^+\Sigma^0] + C$, *Z. Phys. C* 68 (1995) 585)
- **But** also compatible with re-scattering effects close to open and hidden strange thresholds in a region with various hadronic bound states.

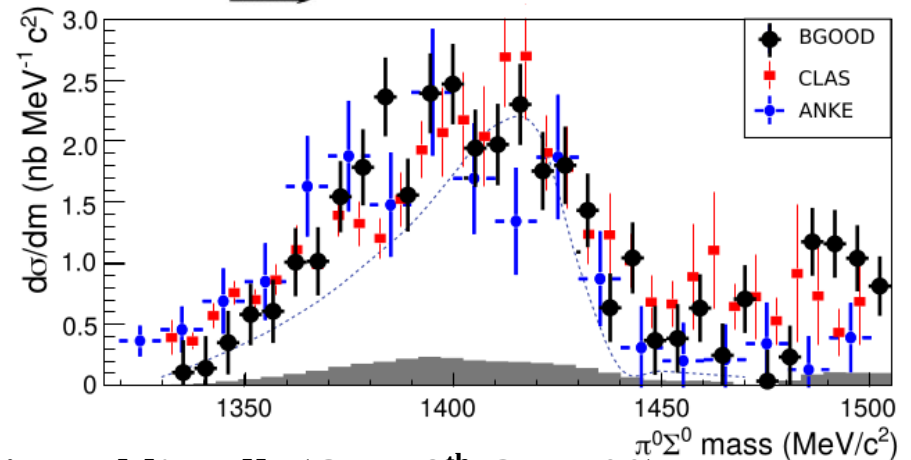
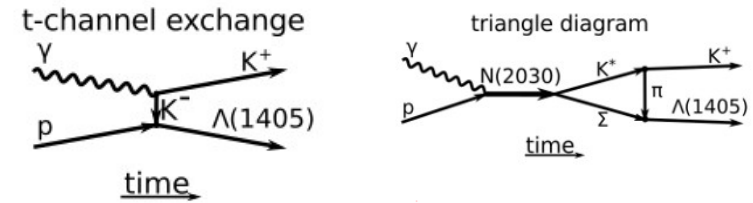
$\gamma p \rightarrow K^+ \Lambda(1405) \rightarrow K^+ \pi^0 \Sigma^0$
 G. Scheluchin, T.C. Jude *et al.*
 Phys. Lett. B 833 (2022), 137375



[CLAS: Moriya, PRC 87, 035206 (2013)]
 [M. Nanova et al., EPJA 35 (2008) 333]



See Katrin Kohl's talk (Oct 18th @ 15:00)



K^+ detected in forward spectrometer and $\Lambda(1405) \rightarrow \Sigma^0 \pi^0 \rightarrow (\gamma \Lambda) (\gamma \gamma) \rightarrow (\gamma \pi p) (\gamma \gamma)$ with 3 γ 's in BGO
 3 charged p.

- **HERMETIC COVERAGE** → allows detection of all final state particles
- **EXTENSION TO VERY FORWARD ANGLES WITH UNPRECEDENTED ENERGY RESOLUTION**

→ $\Lambda(1405)$ is assumed to mainly proceed via the kaon t-channel exchange dominated by small momentum transfer, t , in particular if it has a relatively loosely bound molecular structure.

→ Another proposed mechanism (PRC 95 (2017) 015205) is a triangle singularity driven by the $N^*(2030)$ (bound $K^* \Sigma$) which is expected to vanish once the threshold of free $K^* \Sigma$ production is exceeded.

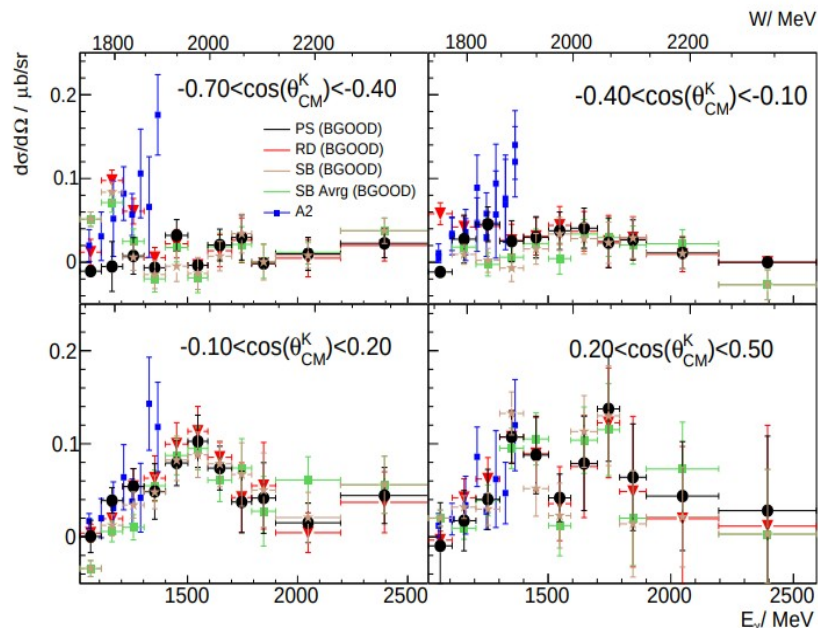
Cross-section data support the triangle mechanism with $N^*(2030)$ (bound $K^* \Sigma$)

- **Measured line-shape of $\Lambda(1405) \rightarrow \Sigma^0 \pi^0$**

$$\gamma n \rightarrow K^0 \Sigma^0$$

K. Kohl *et al.*

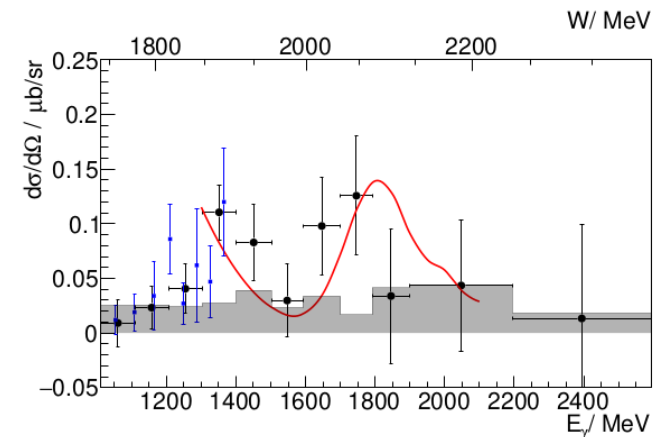
arXiv: 2108.13319 and Submitted to EPJA



blue squares:
C. Akondi, et al. A2,
Eur. Phys. J. A 55,
202 (2019)



See Katrin Kohl's talk
(Oct. 18th @ 15:00)



$$\gamma n \rightarrow K^0 \Sigma^0 \rightarrow (\pi^0 \pi^0) (\gamma \Lambda) \rightarrow (\gamma \gamma \gamma \gamma) (\gamma \pi p)$$

with all γ 's in BGO and most of charged part in BGO/SciFi

- **HERMETIC COVERAGE** → allows detection of all final state particles
- **Structure may become visible @ $0.2 < \cos \theta_{\text{CM}} < 0.5$,**
→ could be interpreted as due to $N^*(2030)$ (dynamically generated $K^* \Sigma$ state) (**Phys. Lett. B 727, (2013) 287**) causing constructive interference between $K^* \Sigma$ and $K^* \Lambda$ states.
N.B. $N^*(2030)$ could also explain the **cusp observed in $K^0 \Sigma^+$** and be responsible for **$\Lambda(1405)$ photoproduction (supported by BGOOD data)**

In principle other interpretations in terms of conventional states cannot be ruled out.

- **Peak at $W = 1900 \text{ MeV}$ @ $-0.10 < \cos \theta_{\text{CM}} < 0.20$ → $\Delta(1900)1/2^-$**

Preliminary Analysis on $\gamma n \rightarrow K^+ \Sigma^- \rightarrow K^+ (\pi^- n)$

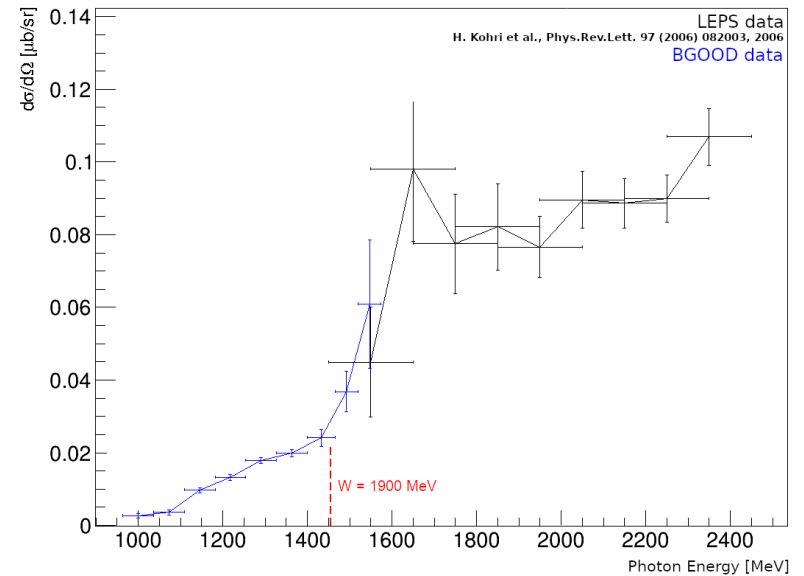
Johannes Groß

➔ See Johannes Groß' talk (Oct 19th@ 15:40)

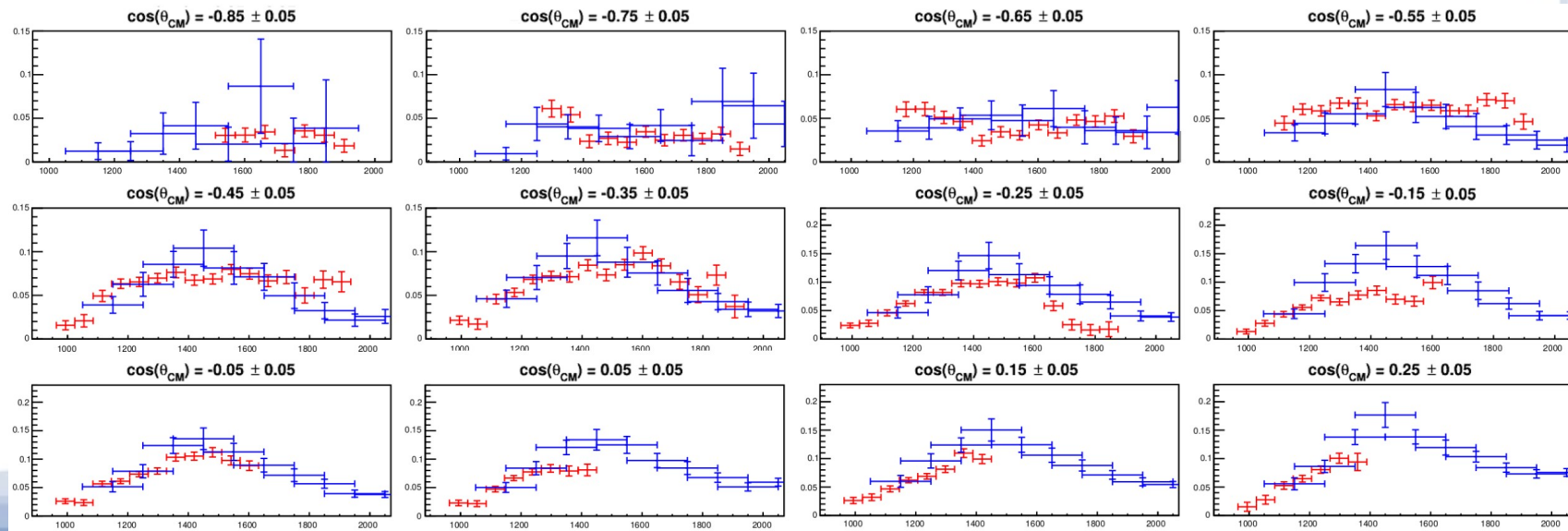
K^+ detected in forward spectrometer
 π^- in BGO
 n not required

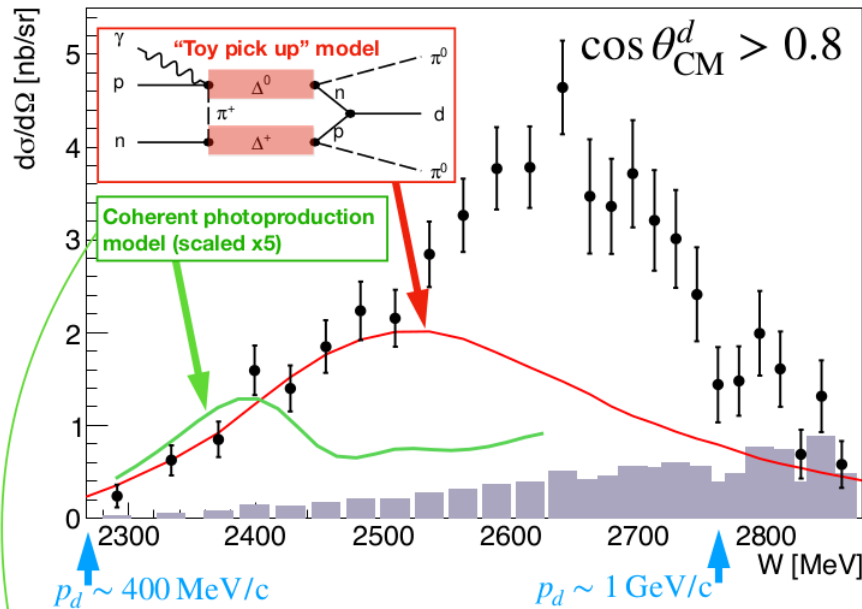
Measured Missing Mass From K^+
 Background from proton subtracted with Hydrogen
 target data

$$\cos\theta_{CM}^{K^+} > 0.9$$

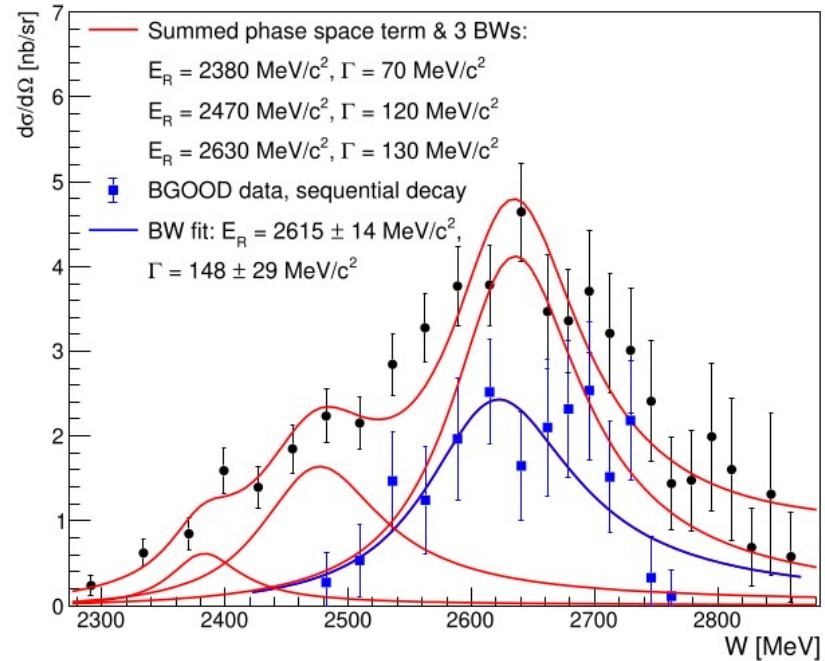


Preliminary data available for K^+ detected in BGO
 $-0.85 < \cos\theta_{CM}^{K^+} < 0.35$





Egorov & Fix, NPA, 933 (2015) 104 - Fix & Arenhövel, EPJA, 25 (2005) 115



➔ See Tom Jude's talk (Oct 18th@ 15:40)

d detected in forward spectrometer and $\pi^0 \pi^0 \rightarrow 4\gamma$'s in BGO $\cos\theta_{CM}^d > 0.8$

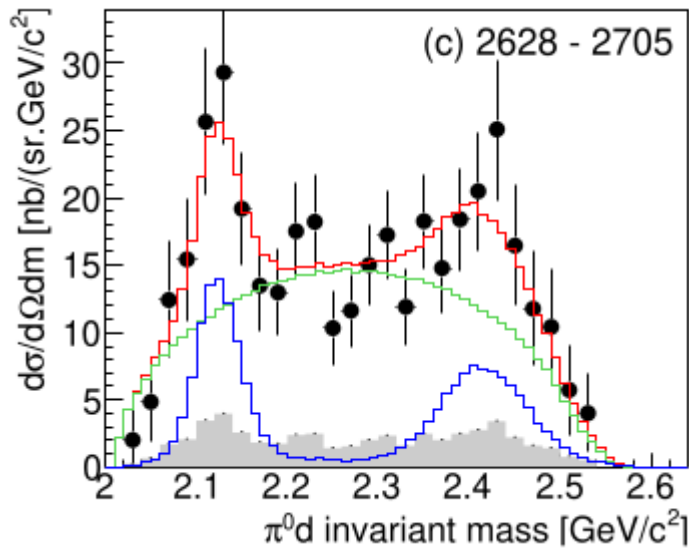
- **X-section peaks at 2650MeV around 4nb/sr**
 - not compatible with coherent photoproduction (**green curve**), "Toy pick-up" models (**red curve**)
 - **compatible** with a 3-isoscalar dibaryon scenario, $d^*(2380)$, 2470 and 2630 MeV/c² reported by ELPH collaboration (PLB 789 (2019) 413) (**red curve, right picture**), but statistics not sufficient to draw conclusions.

- Evidence of $d^*(2380)$ is also supported by the $2\pi^0$ inv. mass confirming the so-called “ABC” effect.

Extracted:



cross section = $(11.3 \pm 3.2_{\text{stat}} \pm 2.7_{\text{sys}})$ nb



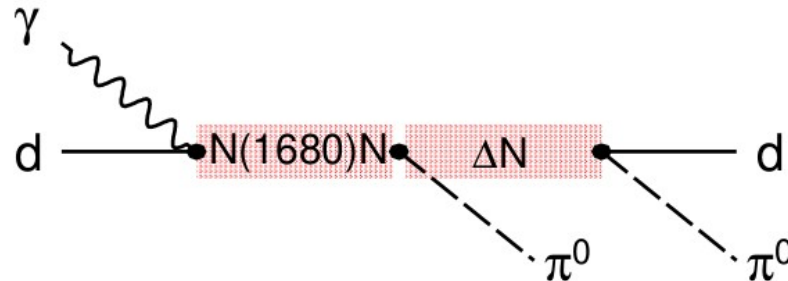
- Double peak structure for $W > 2500$ MeV for $\pi^0 d$ invariant mass, compatible with observations at ELPH of an isovector dibaryon with:

$$M = 2140 \text{ MeV}/c^2 \quad \text{Width} = 91 \text{ MeV}/c^2$$

BGOOD:

$$M = 2117 \text{ MeV}/c^2 \quad \text{Width} = 20 \text{ MeV}/c$$

The isovector is produced via a sequential decay mechanism isoscalar-isovector.



BEAM ASYMMETRY IN MESON PHOTOPRODUCTION

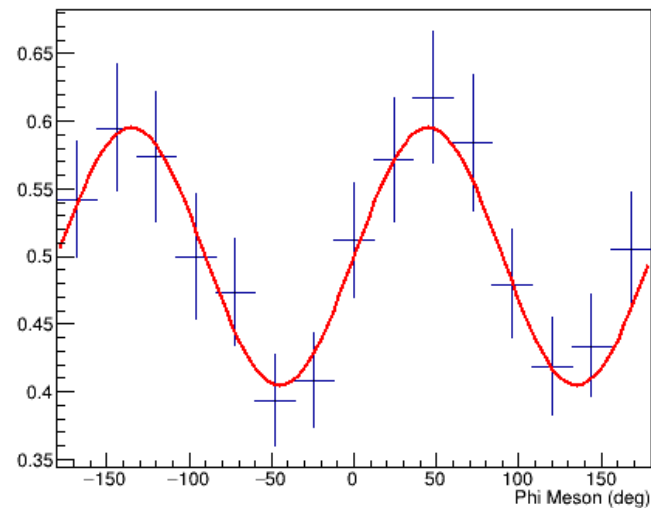
With two polarization states \rightarrow systematical errors not depending on the polarization cancel:

$N_{1,2}(E_\gamma, \theta_{\text{C.M.}}) = \# \text{ events in pol } 1/2$

$F_{1,2}(E_\gamma) = \text{flux of photons in pol } 1/2$

$$\frac{\frac{N_{1,2}}{F_1}}{\frac{N_1}{F_1} + \frac{N_2}{F_2}} = \frac{1}{2} (1 \pm P_\gamma(E_\gamma) \Sigma \cos(2\varphi))$$

$$\Sigma = \Sigma(E_\gamma, \theta_{\text{C.M.}})$$



Extraction of the asymmetry

In the hypothesis that the two polarization states have different degrees of polarization, we have:

$$N_{Pol+}^P = F_{Pol+}^P \left(\frac{d\sigma}{d\Omega} \right)_{UNP} \varepsilon(\varphi) N_{SC} \left(1 + P_{Pol+}^P \Sigma \cdot \cos(2\varphi) \right) \quad (1)$$

$$N_{Pol-}^P = F_{Pol-}^P \left(\frac{d\sigma}{d\Omega} \right)_{UNP} \varepsilon(\varphi) N_{SC} \left(1 - P_{Pol-}^P \Sigma \cdot \cos(2\varphi) \right) \quad (2)$$

$P = \text{period}$

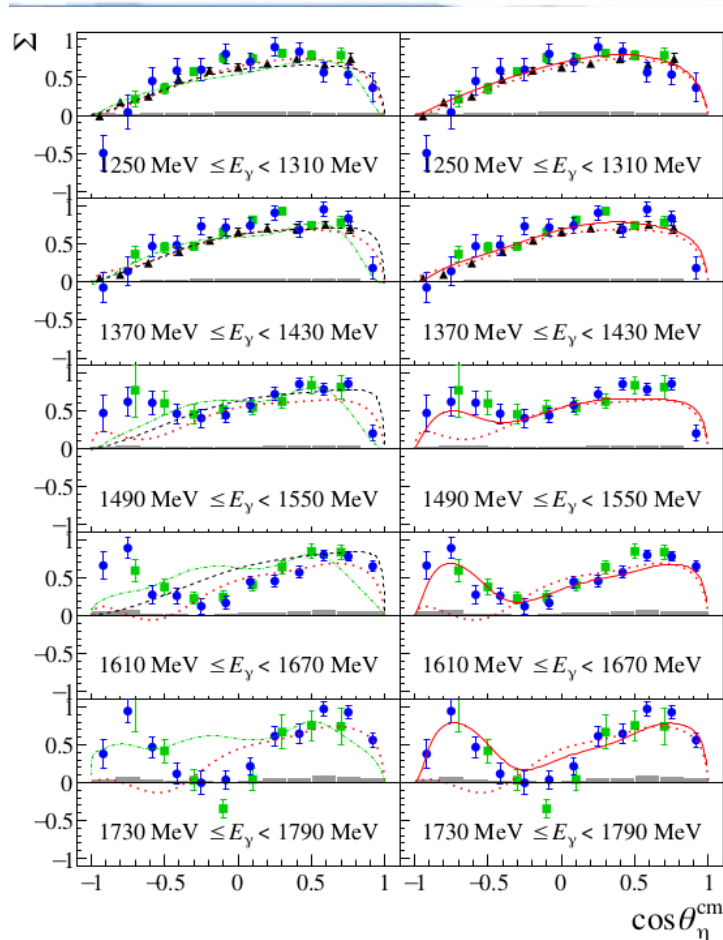
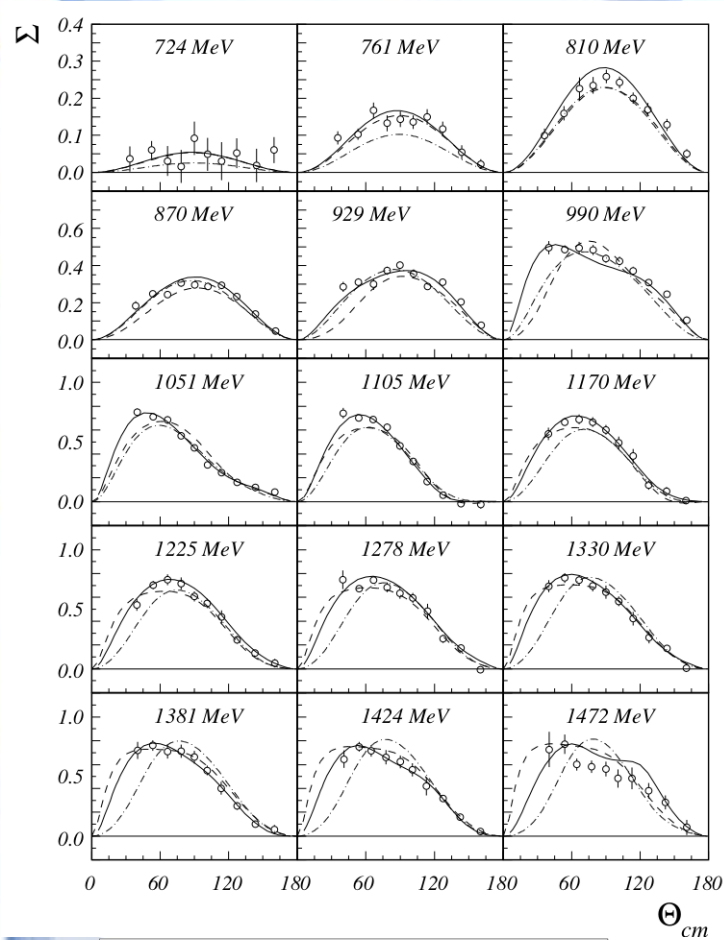
If we extract the asymmetry from the usual ratio:

$$\frac{\frac{N_{Pol+}^P}{F_{Pol+}^P}}{\frac{N_{Pol+}^P}{F_{Pol+}^P} + \frac{N_{Pol-}^P}{F_{Pol-}^P}} = \frac{1 + P_{Pol+}^P \Sigma \cdot \cos(2\varphi)}{2 + (P_{Pol+}^P - P_{Pol-}^P) \Sigma \cdot \cos(2\varphi)} \quad (3)$$

We get a behaviour which depends on phi also in the denominator. This depends on the fact that the denominator is not proportional to the unpolarized cross section.

The unpolarized can be defined as:

$$\frac{N_{UNP}^P}{F_{UNP}^P} = \frac{1}{2} \frac{1}{P_{Pol+}^P + P_{Pol-}^P} \left(P_{Pol-}^P \frac{N_{Pol+}^P}{F_{Pol+}^P} + P_{Pol+}^P \frac{N_{Pol-}^P}{F_{Pol-}^P} \right) \quad (4)$$

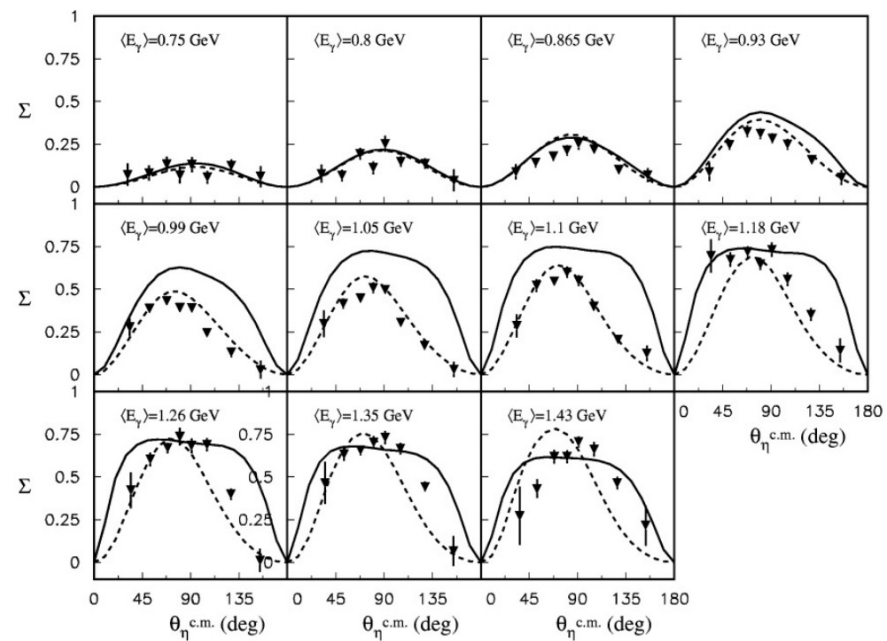


$\gamma p \rightarrow \eta p$
 Blue circles
 PRL 125 (2020) 15,
 152002
 Green squares
 PLB 771, 213 (2017)

$\gamma p \rightarrow \eta p$
 EPJA 33, 169–184 (2007)

Low energy:
 Interf $S_{11}(1535)$ - $D_{13}(1520)$ ($\sin^2 \theta_{\eta}^{cm}$ behav.)
High energy: interference $S_{11}(1535)$ - $F_{15}(1680)$
 (peak at forward angles)

$\gamma n \rightarrow \eta n$
 Full triangles
 PRC78 (2008) 015203



$\gamma p \rightarrow \eta p$

Preliminary

R. Di Salvo, A. Fantini, P. Levi Sandri

Analysed reactions

1) $\eta \rightarrow 2 \gamma$

with: 2 γ in BGO + 1 proton in all detector

2) $\eta \rightarrow 3\pi^0 \rightarrow 6 \gamma$

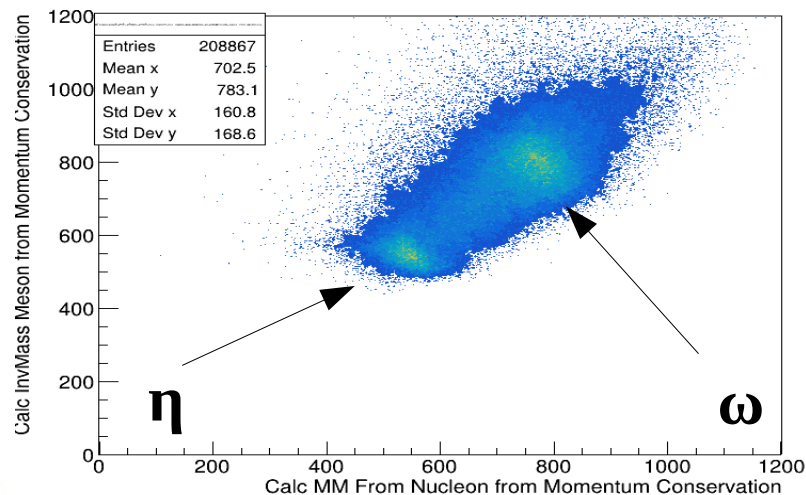
with: 6 γ in BGO + 1 proton in all detector

3) $\eta \rightarrow \pi^+\pi^-\pi^0$

with 2 γ in BGO + 1 proton in all detector + $\pi^+\pi^-$ in BGO

→ proton and charged pions momenta reconstructed from momentum conservation between initial and final state particles with no hypothesis on the decaying meson

Reconstructed
Inv. Mass ($\pi^+\pi^-\pi^0$)

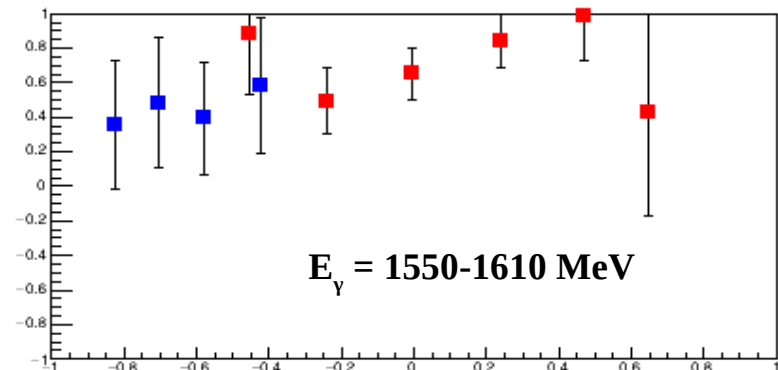
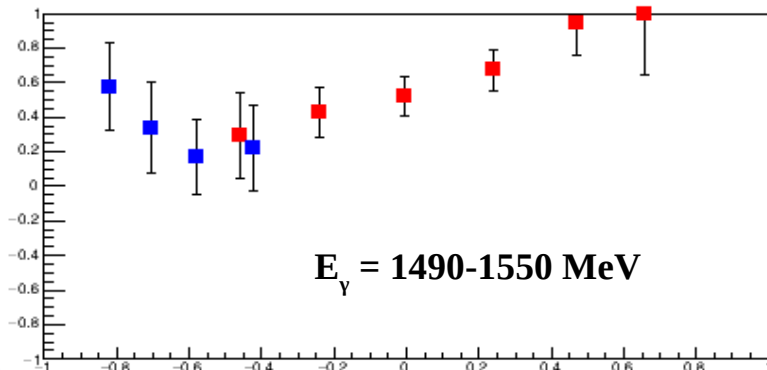
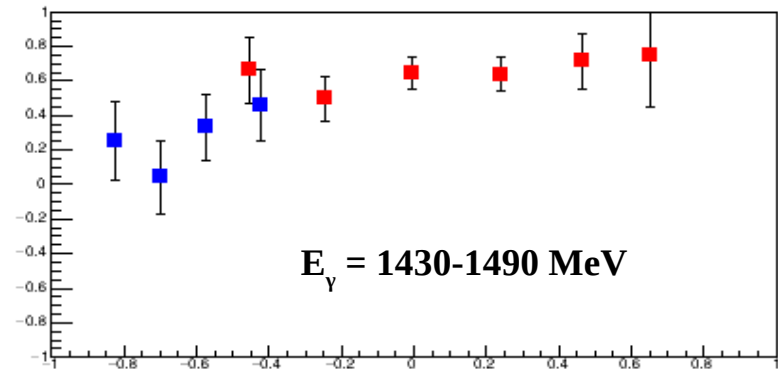
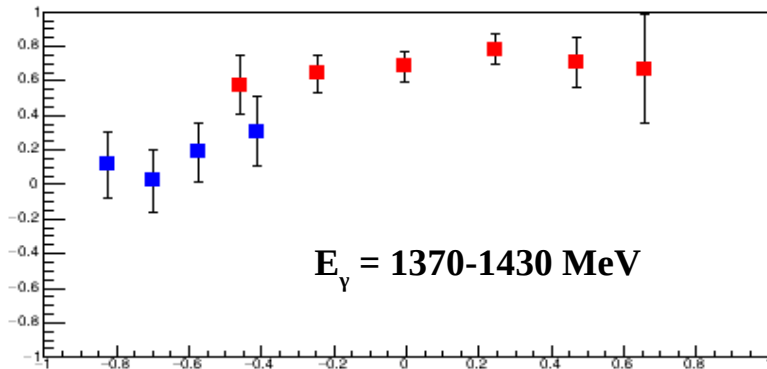
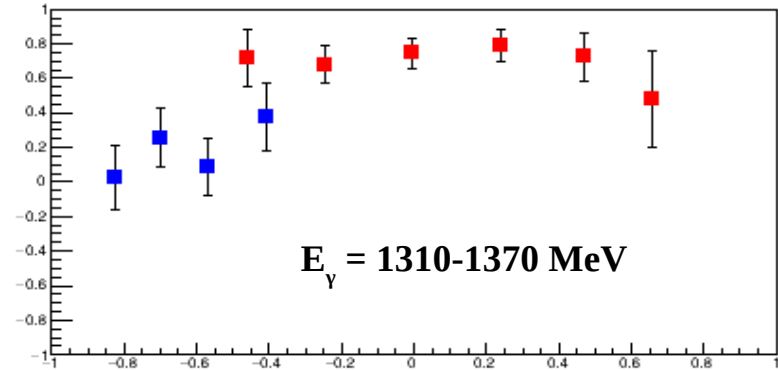
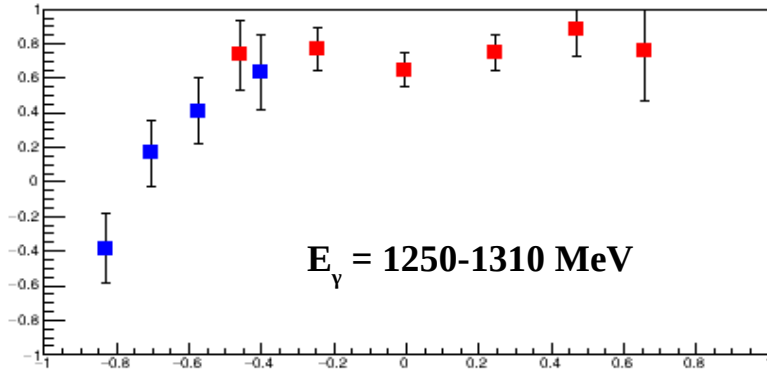


Reconstructed
Miss Mass from Proton

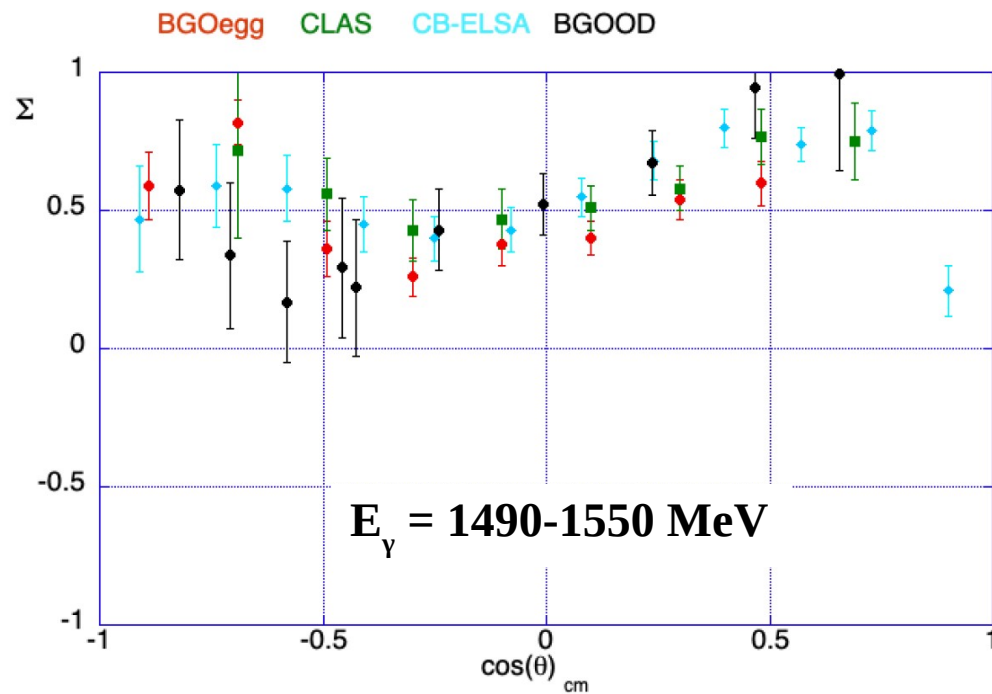
AprMay2017+NovDec2018 $\eta \rightarrow 2\gamma, 6\gamma, \pi^+\pi^-\pi^0$

Blue Points = Proton in SciRi
 Red Points = Proton in BGO

Squares = PolPlus 15 Bins in ϕ

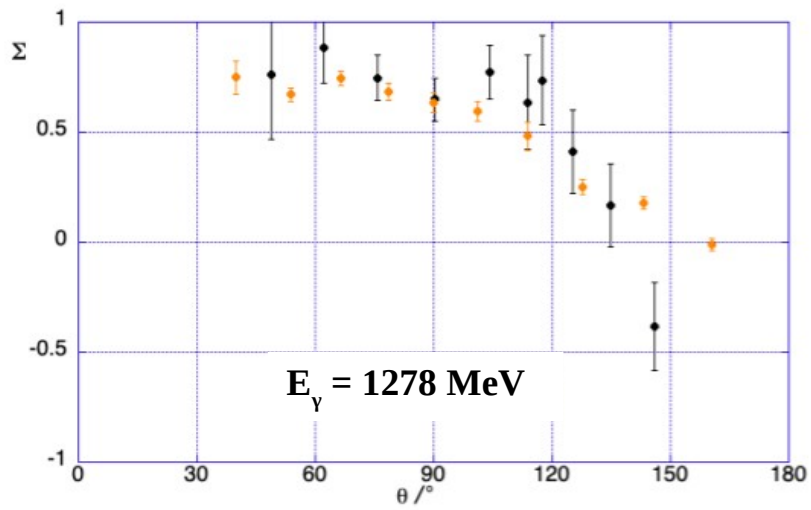


$\gamma p \rightarrow \eta p$

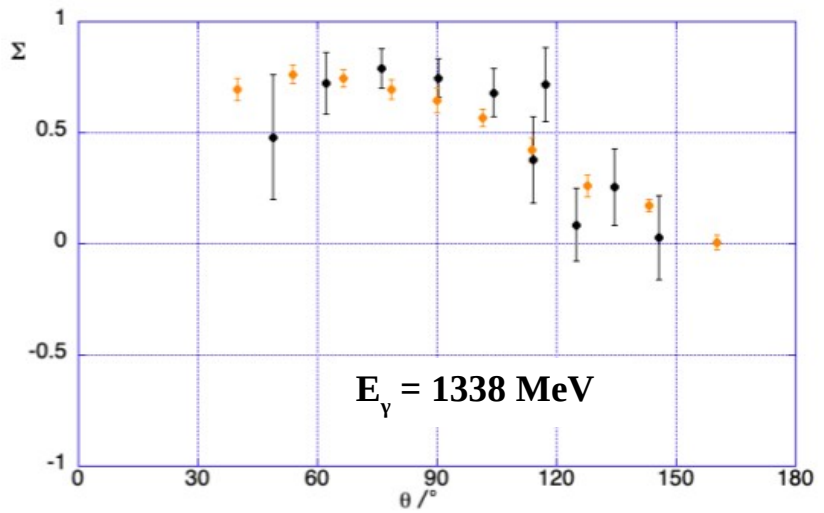


$\gamma p \rightarrow \eta p$

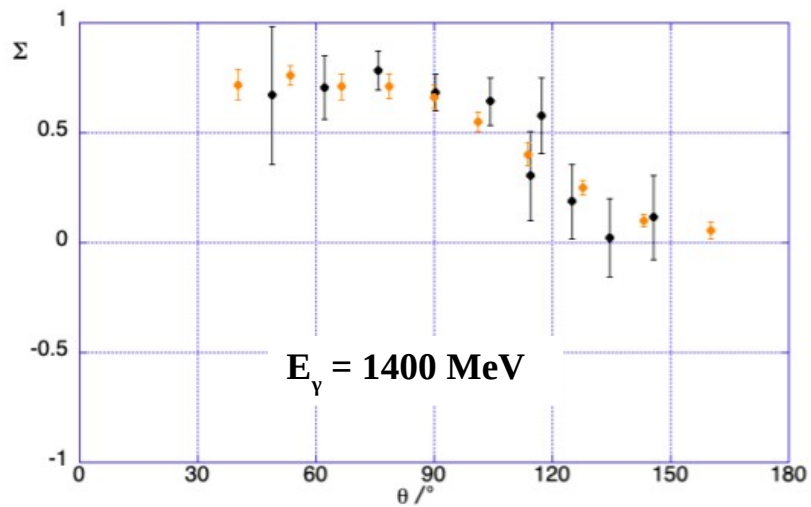
GrAAL E γ 1277 MeV BGOOD Eg 1278 MeV



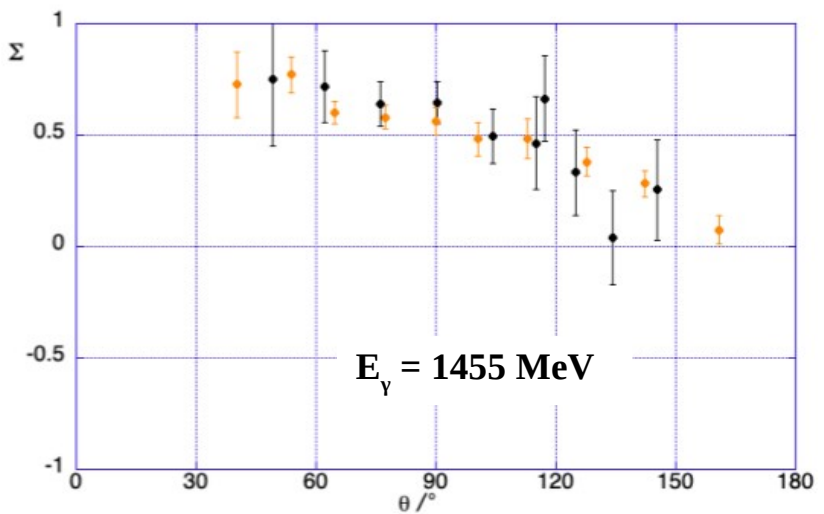
GrAAL E γ 1330 MeV BGOOD Eg 1338 MeV



GrAAL E γ 1381 MeV BGOOD Eg 1400 MeV

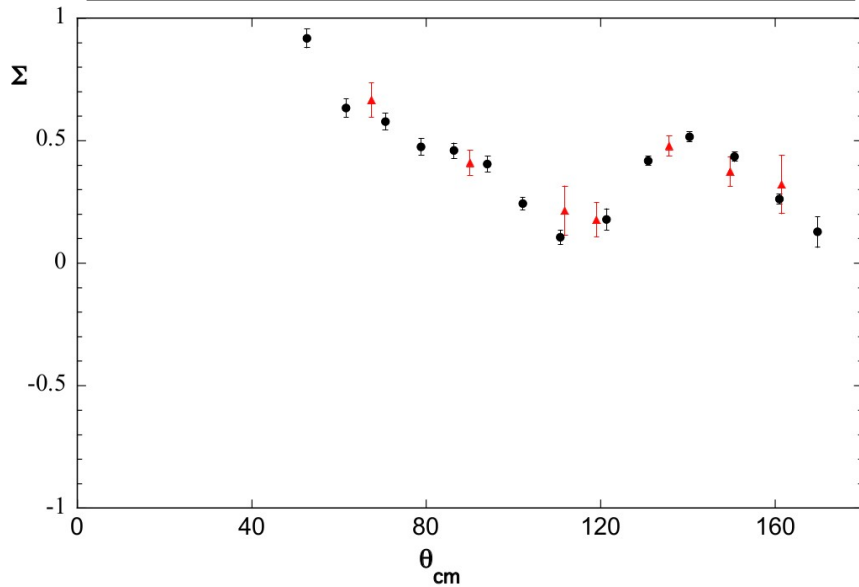


GrAAL E γ 1472 MeV BGOOD Eg 1455 MeV

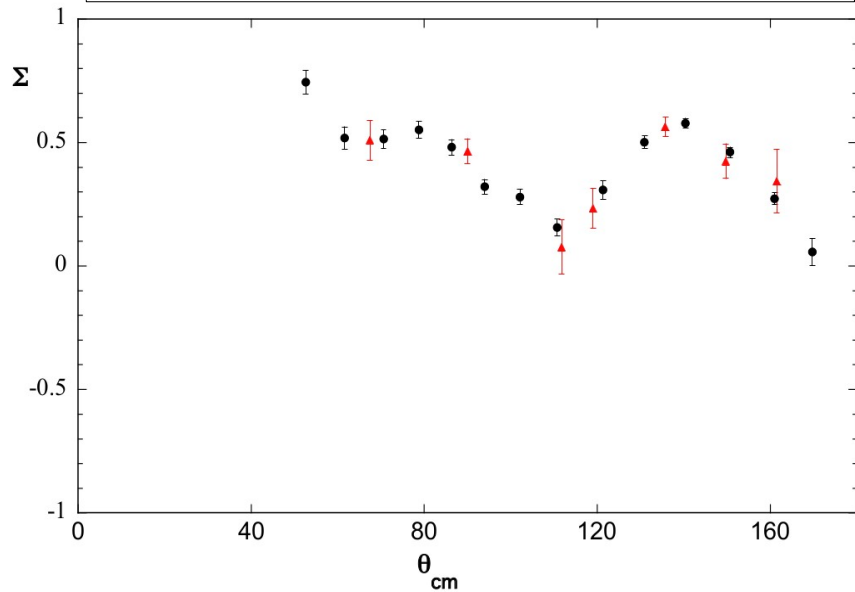


$\gamma p \rightarrow \pi^0 p$

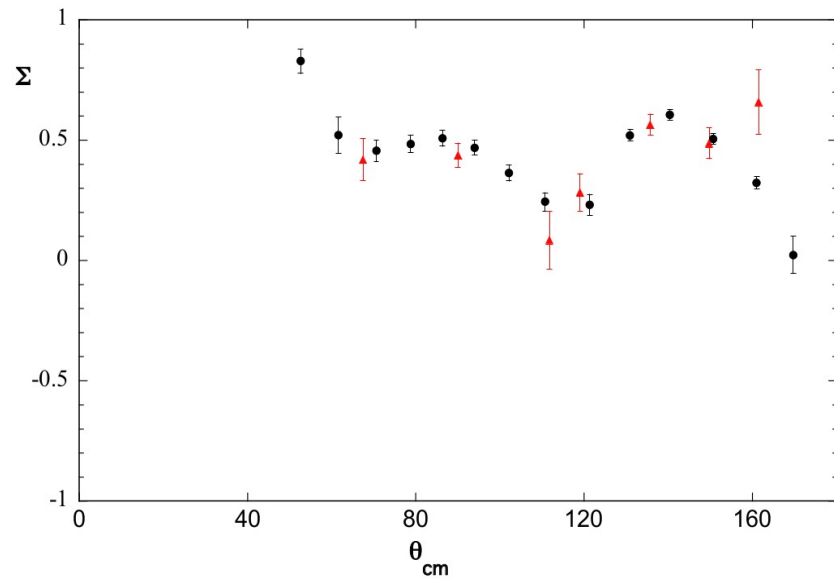
Black Points GRAAL $E_\gamma = 1425$ MeV
Red Triangles BGOOD $E_\gamma = 1425$ MeV



Black Points GRAAL $E_\gamma = 1450$ MeV
Red Triangles BGOOD $E_\gamma = 1450$ MeV



Black Points GRAAL $E_\gamma = 1475$ MeV
Red Triangles BGOOD $E_\gamma = 1475$ MeV

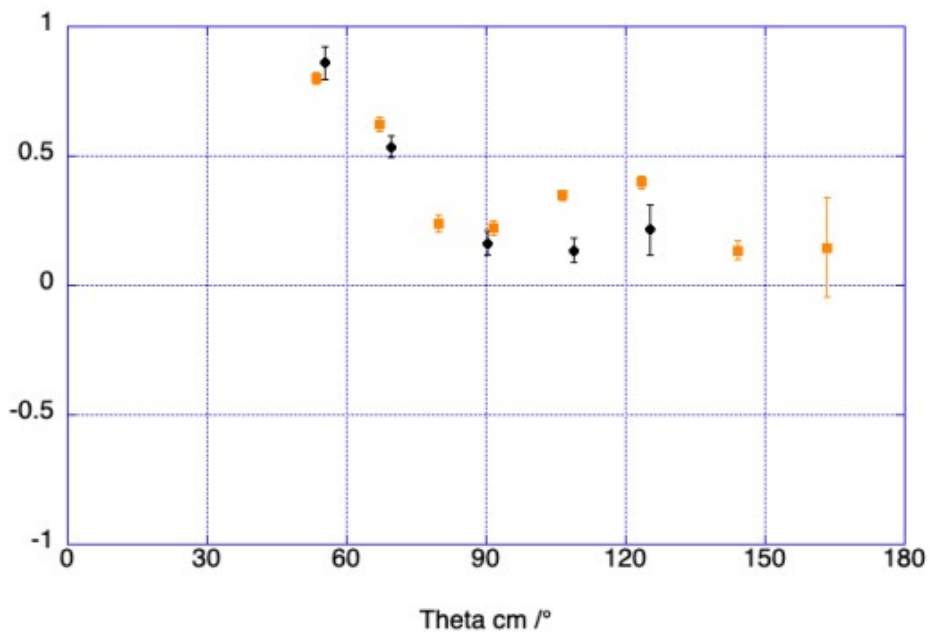


STL

$\gamma n \rightarrow \pi^0 n$

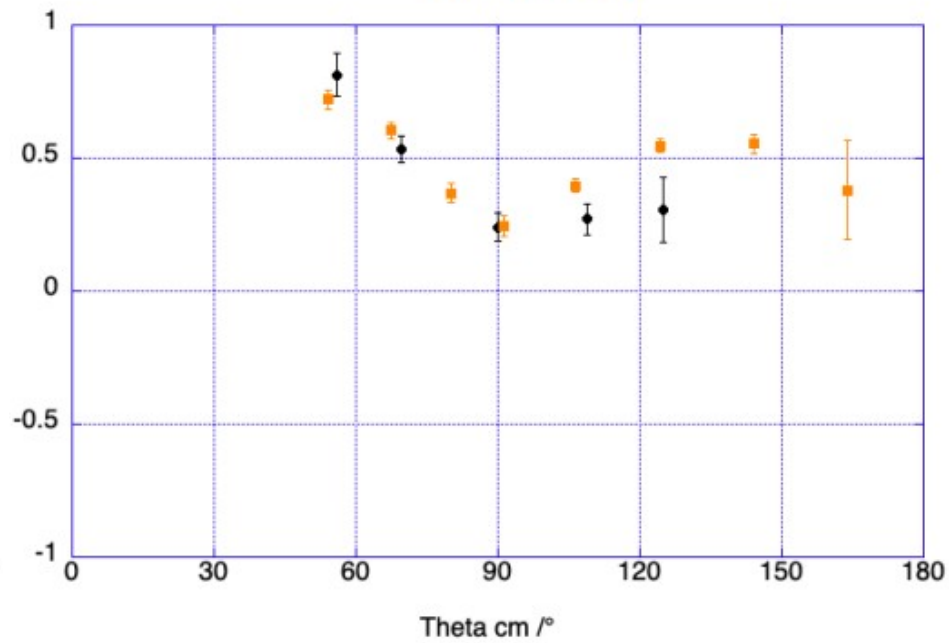
BGOOD $E_\gamma=1108$

GrAAL $E_\gamma=1113$



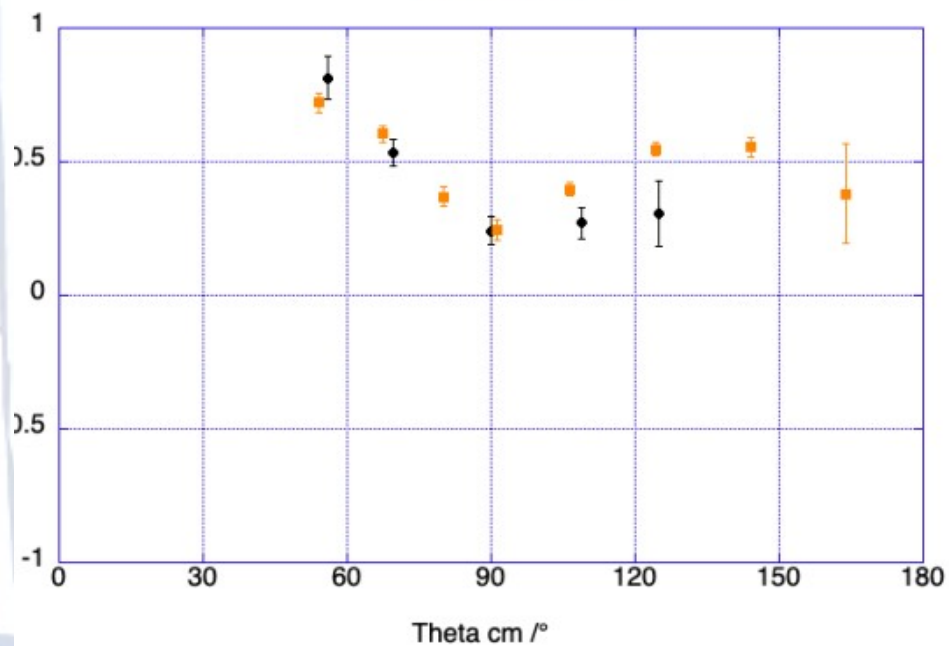
BGOOD $E_\gamma=1270$

GrAAL $E_\gamma=1288$



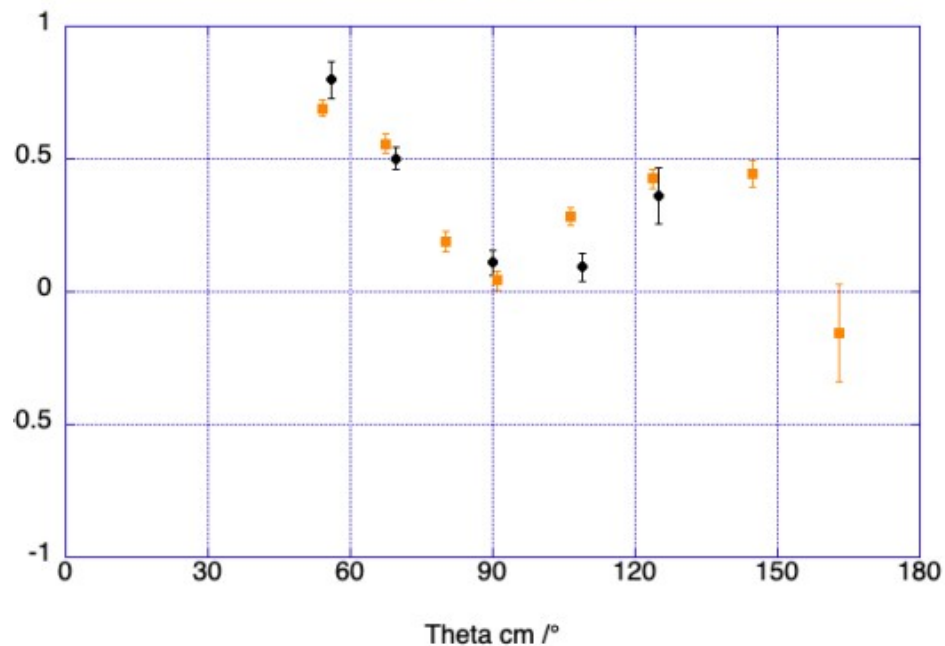
BGOOD $E_\gamma=1270$

GrAAL $E_\gamma=1288$



BGOOD $E_\gamma=1190$

GrAAL $E_\gamma=1202$



SUMMARY AND CONCLUSIONS

- BGOOD is a unique detector for forward acceptance and hermetic coverage working in the 3rd resonance region.

- An extensive program in progress at BGOOD on:
strangeness photoproduction focused on forward angles and low momentum transfer → **potential to investigate unconventional states**

$$\gamma p \rightarrow K^+ \Lambda, K^+ \Sigma^0, K^+ \Lambda(1405)$$

$$\gamma n \rightarrow K^0 \Sigma^0, K^+ \Sigma^-$$

baryon-baryon dynamics in the ud sector

$$\gamma p \rightarrow d \pi^0 \pi^0, d \pi^0 \pi^0 \pi^0, d \eta \pi^0$$

pseudoscalar meson photoproduction on proton and neutron (and also vector mesons ω in the future)

- Improving the statistics of some channels (also already published) is possible.
Statistics to be analyzed is already available on tapes.

THANK YOU!!

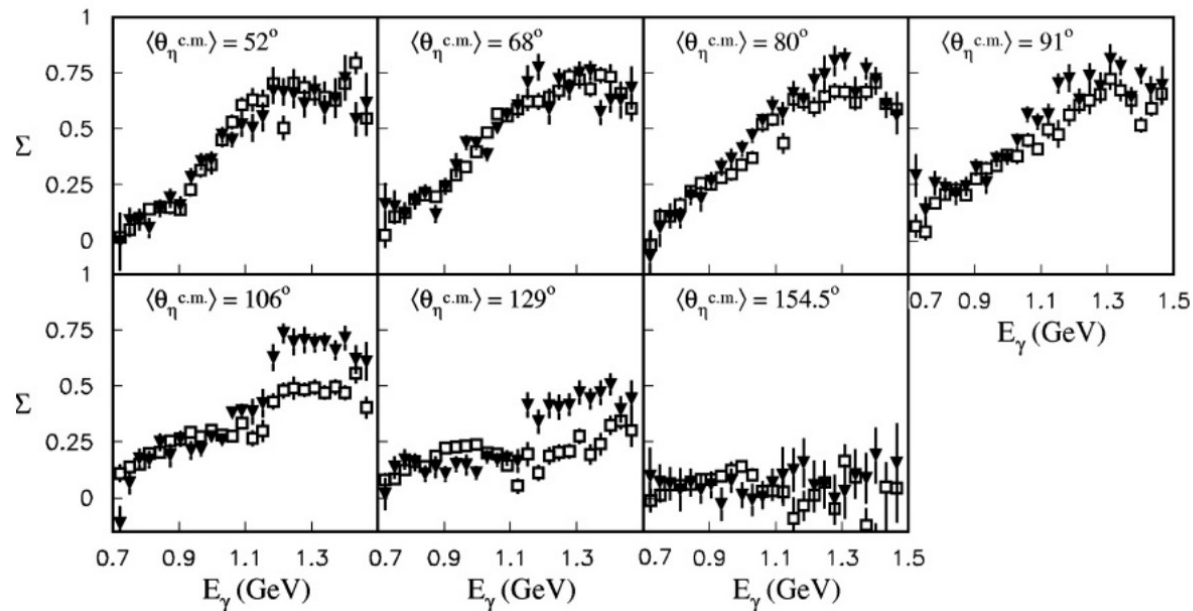
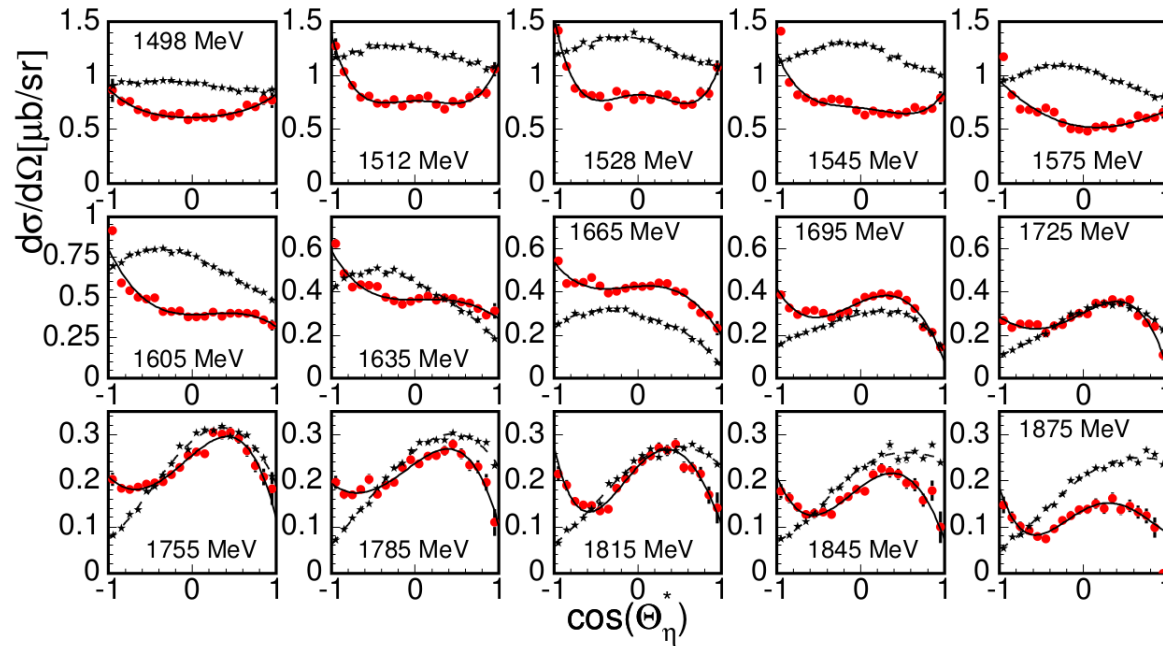
BACKUP SLIDES

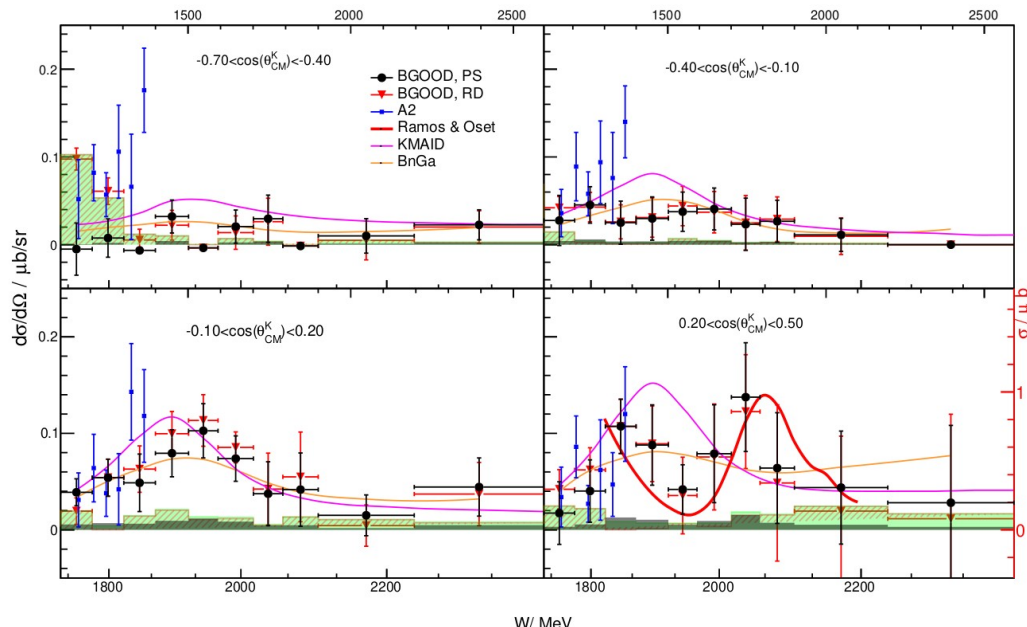
EXPERIMENTAL SITUATION FOR η PHOTOPRODUCTION

$\gamma p \rightarrow \eta p$
 Black Pts
 PRC82 (2010) 035208

$\gamma n \rightarrow \eta n$
 Red Pts
 PRL111 (2013) 232001

$\gamma p \rightarrow \eta p$
 Open Squares
 $\gamma n \rightarrow \eta n$
 Full triangles
 PRC78 (2008) 015203





See Katrin Kohl's talk
(Oct. 18th @ 15:00)

$\gamma n \rightarrow K^0 \Sigma^0 \rightarrow (\pi^0 \pi^0) (\gamma \Lambda) \rightarrow (\gamma \gamma \gamma \gamma) (\gamma \pi p)$

with all γ 's in BGO and most of charged part in BGO/SciFi

HERMETIC COVERAGE

→ allows detection of all final state particles

Structure may become visible at $0.2 < \cos \theta_{CM} < 0.5$,

→ could be interpreted as due to a vector meson-baryon dynamically generated $K^* \Sigma$ resonance, the $N^*(2030)$ (*Phys. Lett. B* 727, (2013) 287) causing the constructive interference between $K^* \Sigma$ and $K^* \Lambda$ states.

N.B.

- In the same model $N^*(2030)$ could explain a **cusp observed in $K^0 \Sigma^+$** (destructive interference between $K^* \Lambda$ and $K^* \Sigma$ states amplified by $N^*(2030)$).

- $N^*(2030)$ is supported by BGOOD data in $\Lambda(1405)$ photoproduction

In principle other interpretations in terms of conventional states cannot be ruled out.



Trends in particle and nuclei identification techniques in nuclear physics experiments

7.3 BGOOD (MAMBO): neutral particles discrimination with BGO

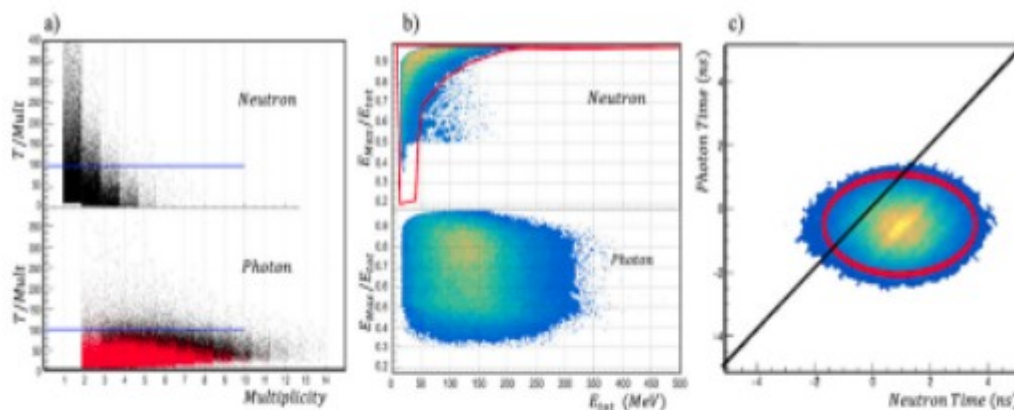


Fig. 35 MAMBO. **a** Ratio between the total cluster energy and the cluster multiplicity for neutrons and photons (in black and red the more and less energetic π^0 decay photons, respectively). **b** Ratio between the maximum energy released in a crystal and the total cluster energy for neutrons with multiplicity > 2 and photons (sum of red and black distributions from **a**). The applied graphical cut is the red contour. **c** photon TOF versus neutron TOF distribution for selected events, the applied cut is presented in red. Ambiguity between two neutral signals with the same multiplicity is solved assigning the neutron tag to the signal with larger TOF (see 45° black line in the picture)

NEUTRON/PHOTON DISCRIMINATION IN BGO

GOAL OF THE JOB

Find criteria for identification and separation neutron/photon in BGO

N.B. Sampling ADC used for BGO crystals readout allow also time measurement with 1.5ns resolution.

TECHNIQUE

Start from a clean sample of selected events with a neutron and a photon in the final state.

The selection is based only on kinematical criteria.

Derive criteria for neutron/photon discrimination from this clean sample.

CHOSEN REACTION: $\gamma n \rightarrow \pi^0 n$

SELECTION CRITERIA:

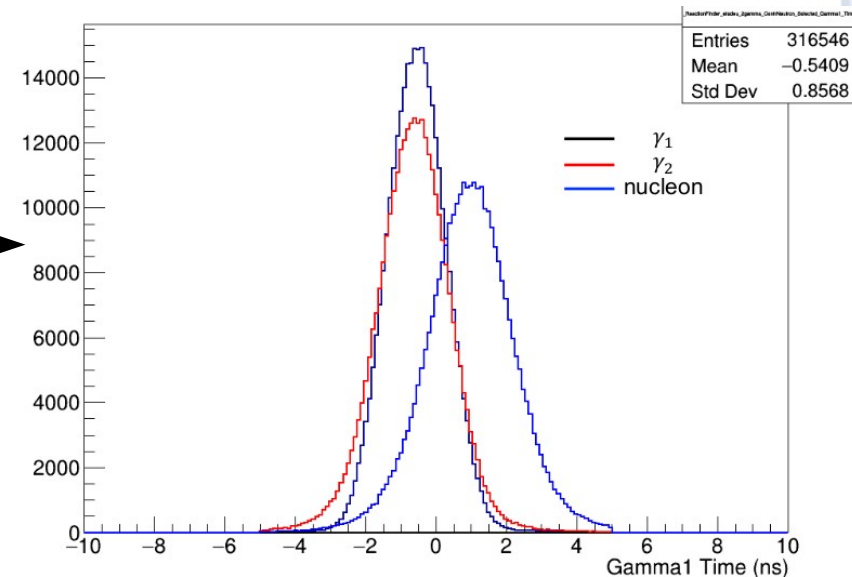
- 3 “neutral” clusters in BGO (i.e. with no signal in barrel/mwpc in geometrical coincidence), arranged into 3 possible combinations

- Choose the combination for which neutron cluster has the lowest multiplicity Mult or, being Mult equal, the largest ToF

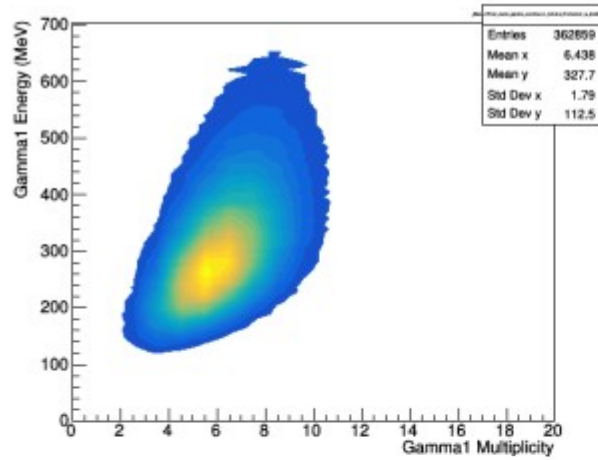
(in average nucleon tof > γ ToF)

- Kinematical cuts on the 2-body reaction

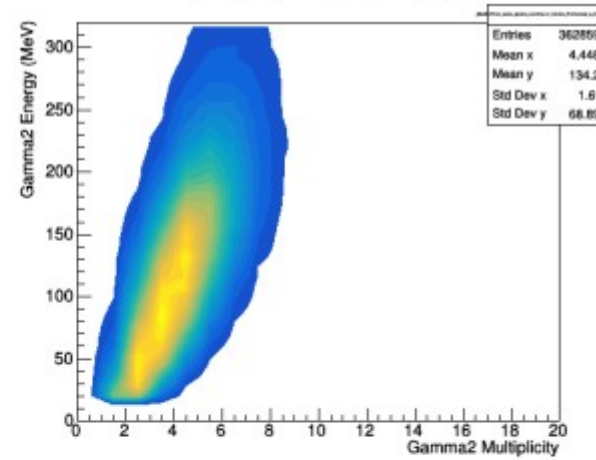
R. Di Salvo - NSTAR22 - Oct. :



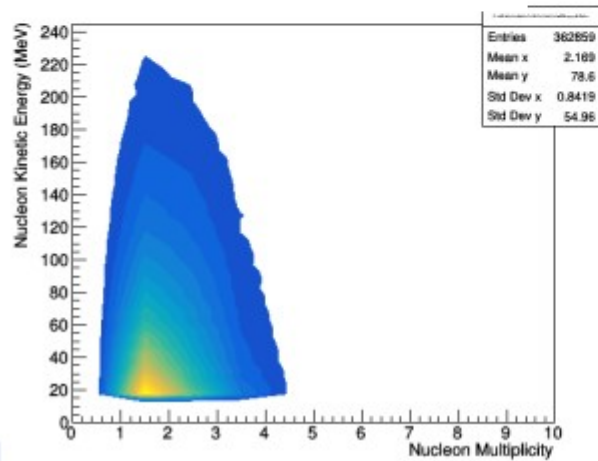
HIGH ENERGY PHOTONS



LOW ENERGY PHOTONS



NEUTRONS



PID CRITERIA:

1) Ratio between the cluster total energy and cluster multipl:

$$R = \frac{ETOT_{Clus}}{Mult_{Clus}}$$

R vs. Mult.

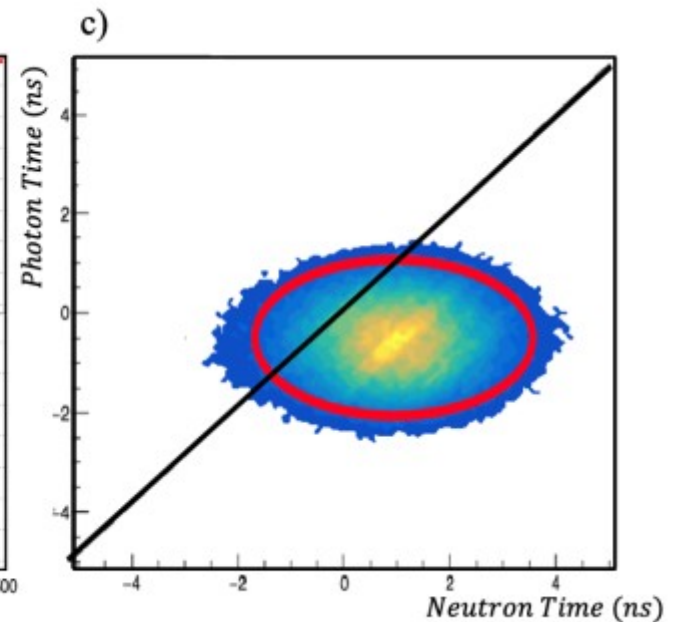
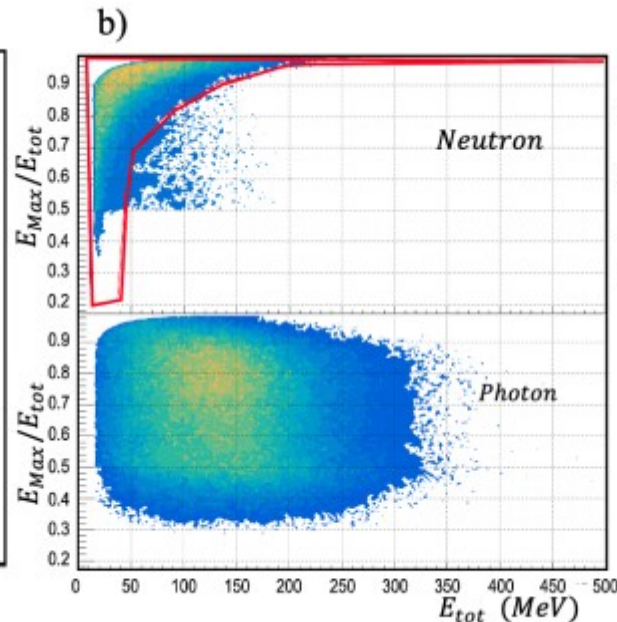
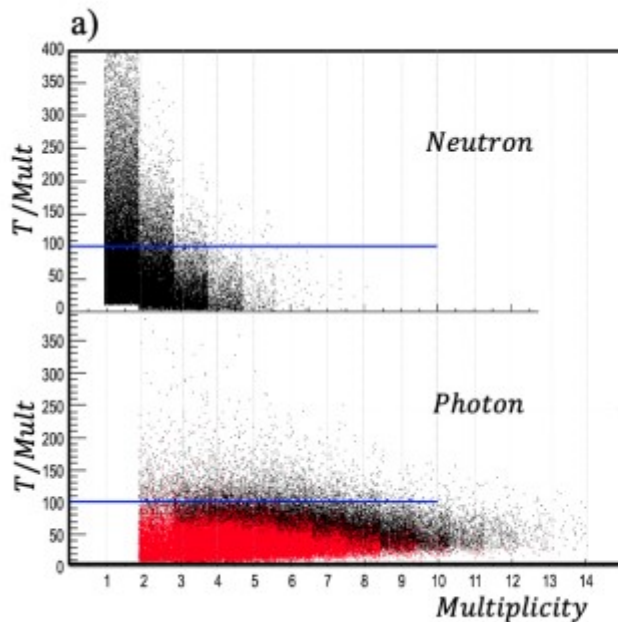
Photons: $R < 100$ MeV/crystal
Neutrons: $R < 400$ MeV/crystal

2) Ratio between the max energy in a crystal of a cluster and the total cluster energy:

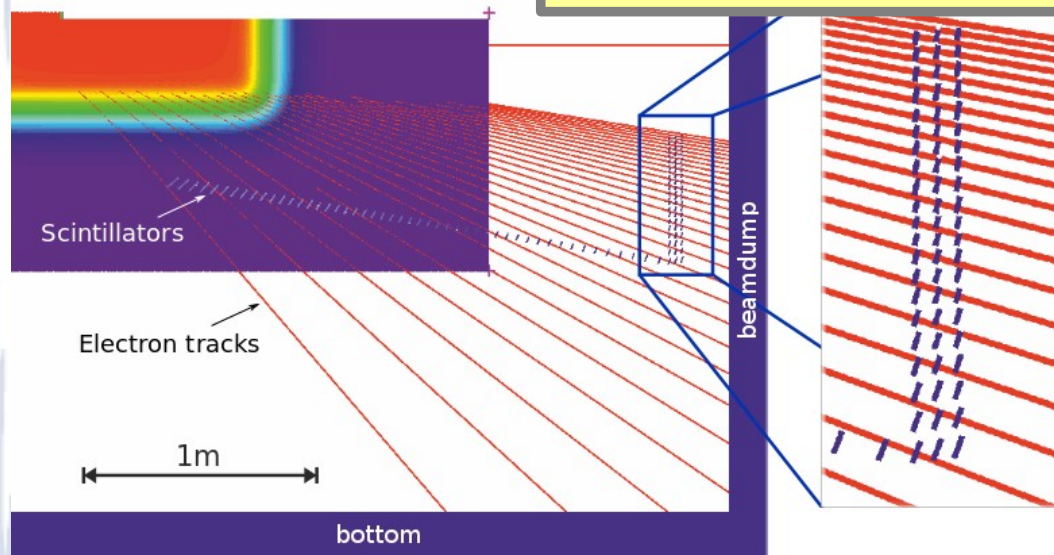
$$R' = \frac{E_{Cryst,MAX}}{ETOT_{Clus}}$$

R' vs. $ETOT_{Clus}$

3) neutron tof (≈ 1 ns) is in average higher than γ (≈ -0.5 ns)



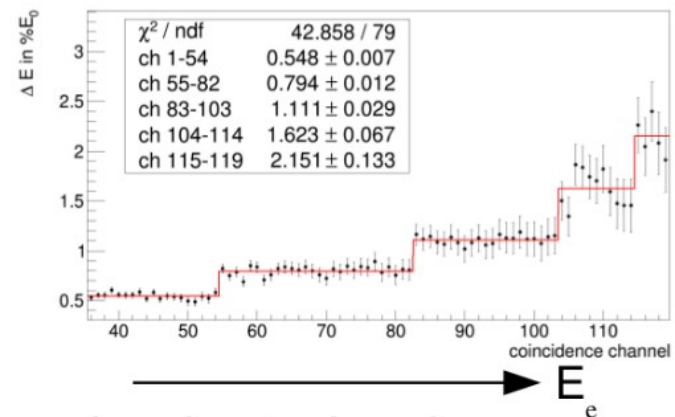
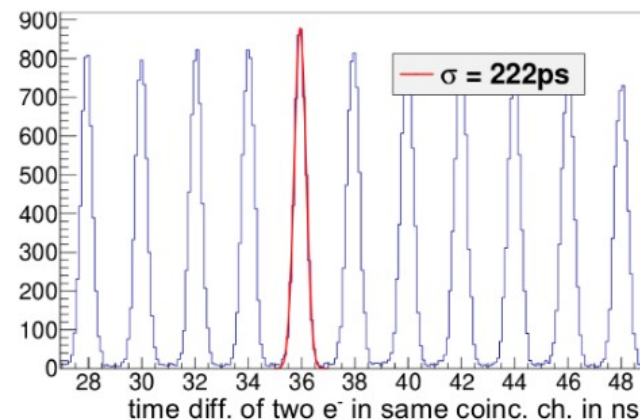
TAGGER DESIGN



Siebke, G.

- High energy e^- (\rightarrow low en. γ): focal plane is not accessible split into 54 horizontal scint. ($10-32\% E_0$) and 66 vertical ones ($32-90\% E_0$)
- trigger on double and triple coincidences

- 120 Channels (covering $0.1-0.9 E_0$)
- Energy resolution: 10-40 MeV ($0.55\% E_0 - 2.15\% E_0$)
- Beam Intensity: $5 \cdot 10^7 s^{-1}$

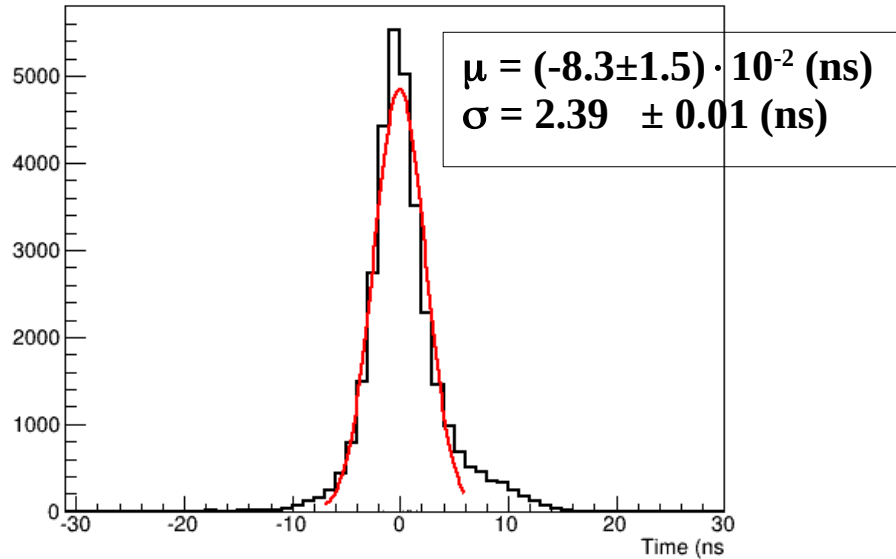


R. Di Salvo - NSTAR22 - Oct. 20th, 20

Time Distribution of clusters in BGO

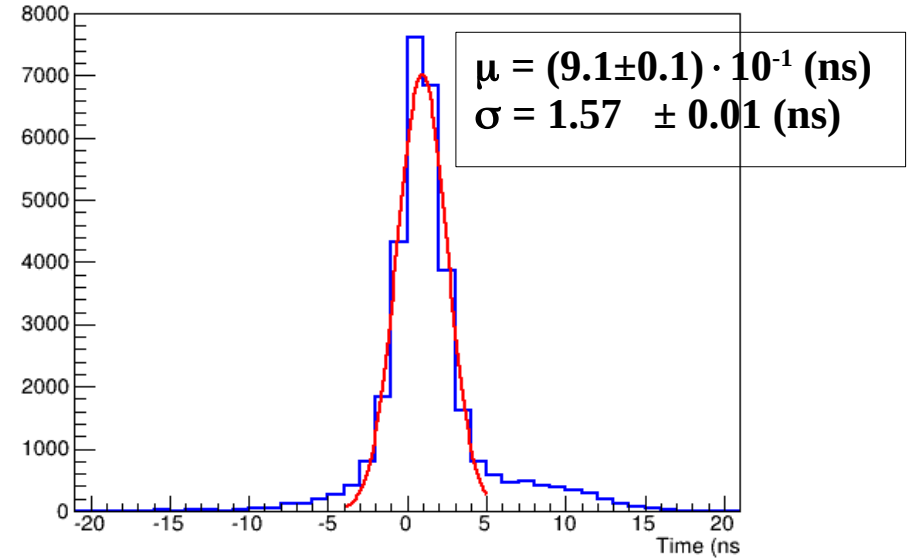
Clusters from a photon

For selected π^0 events

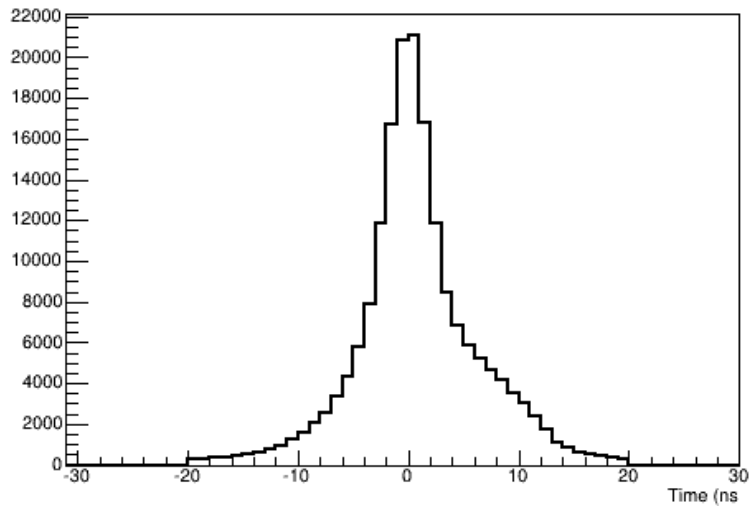


Clusters from a proton

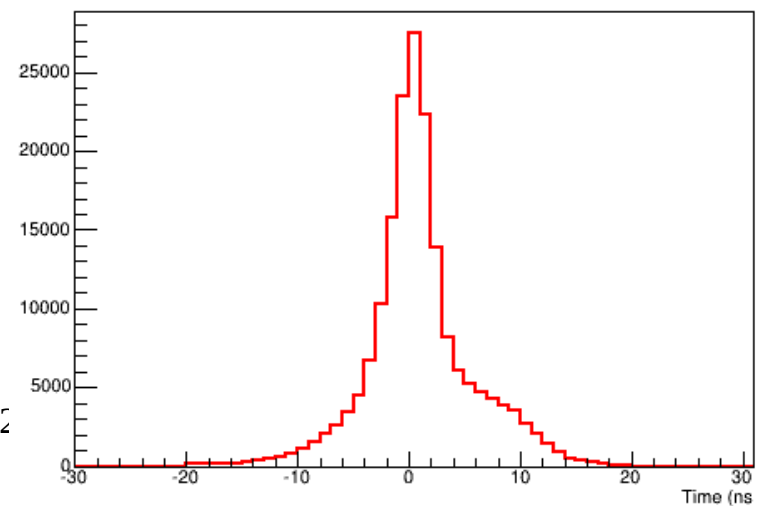
For selected π^0 events



For not selected events



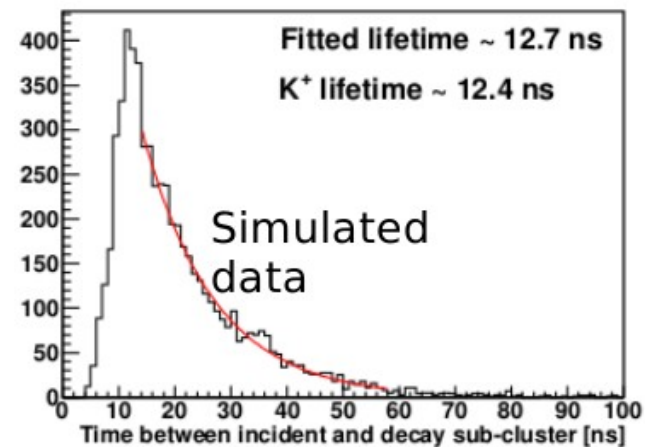
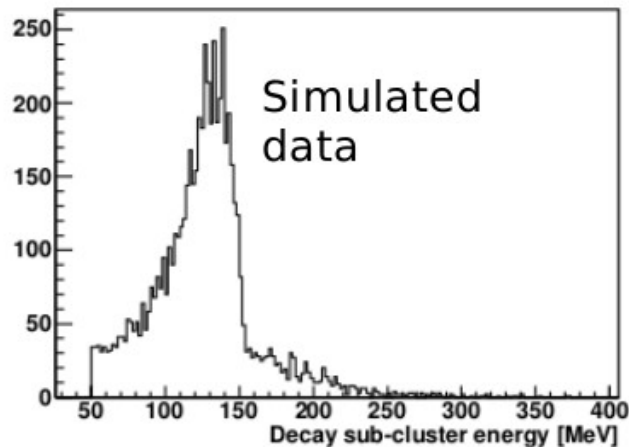
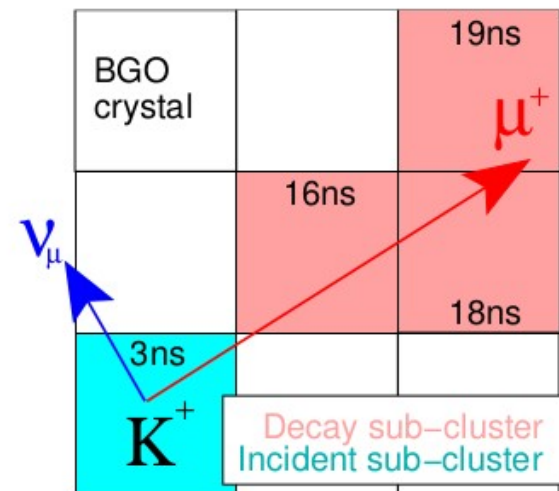
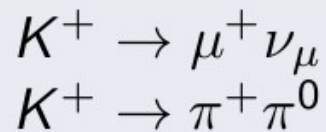
For not selected events



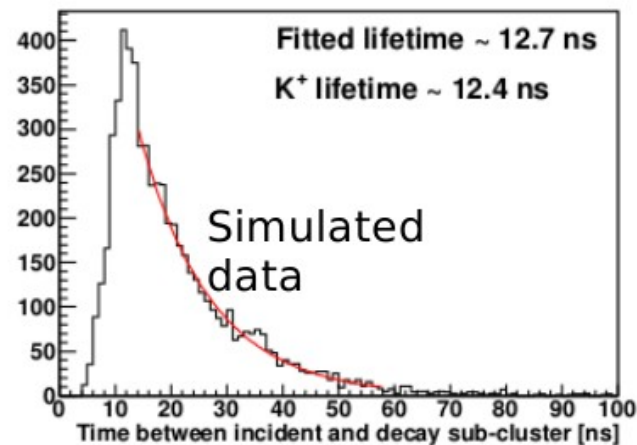
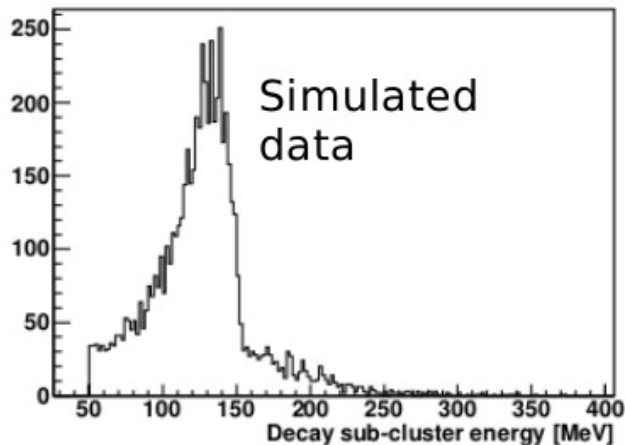
K^+ identification with the BGO ball

- Time delayed, K^+ weak decay within the crystals of the BGO ball
- Technique proven with the Crystal Ball, Mainz

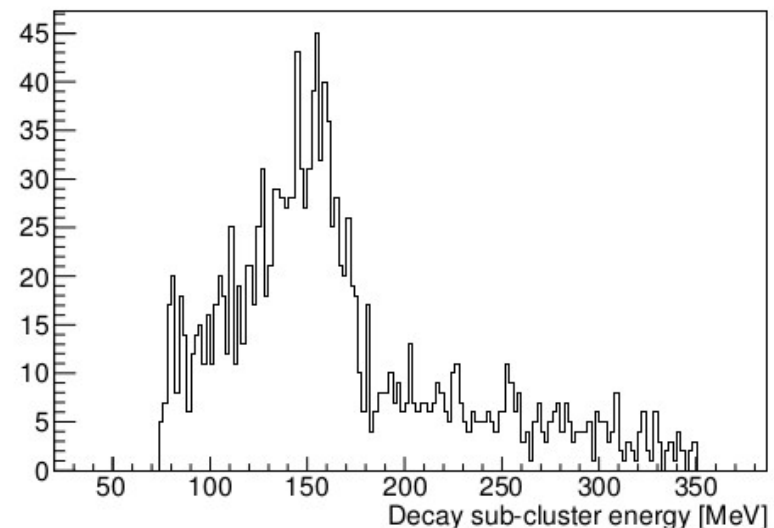
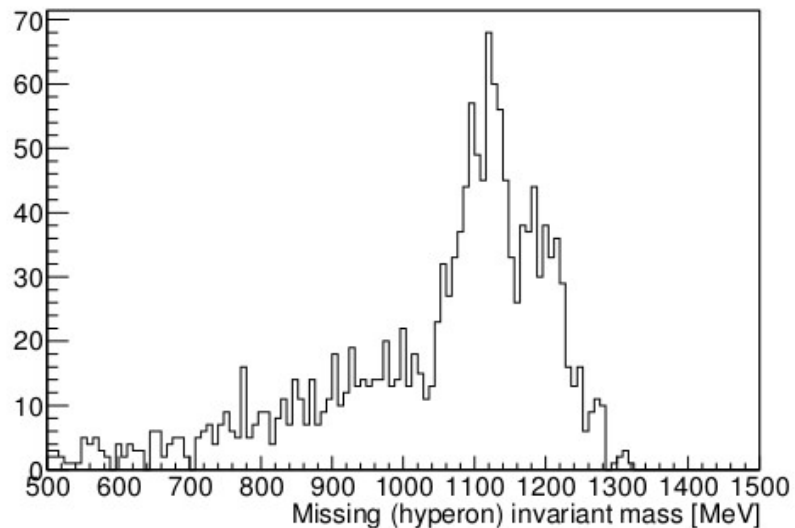
Lifetime 12 ns,
2 main decay modes:



K^+ identification with the BGO ball



- Preliminary experimental data (no charged particle ID used):

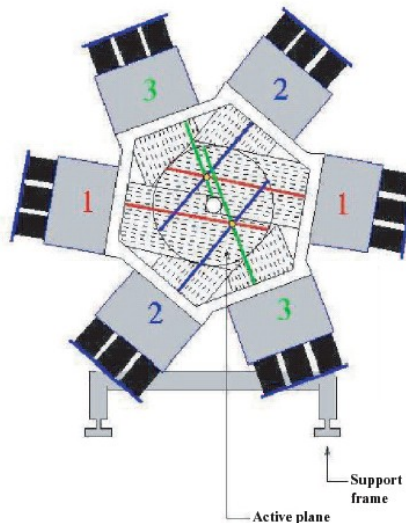


FORWARD SPECTROMETER: BEFORE DIPOLE

MOMO

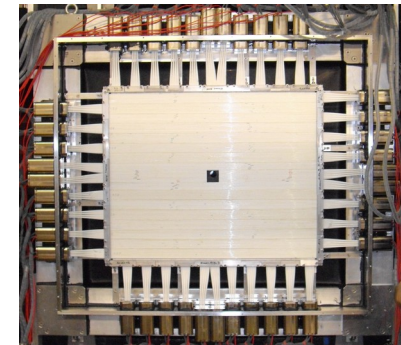
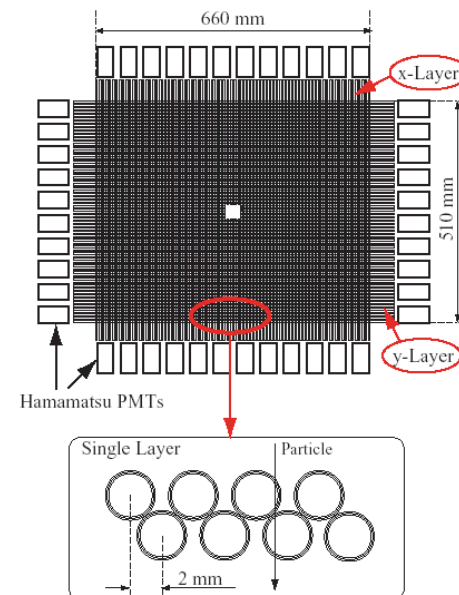
Successful commissioning with beam tests in Feb.-March 2012 and June 2012

Scintillation fiber detector ($\varnothing 44\text{cm}$)
672 total channels
3 layers of 2x112 parallel fibers
($\varnothing 2.5\text{mm}$, $\Delta x = 1.5\text{mm}$)
Each layer rotated of 60° w.r.t. each other
Read-out 16 channel PM
Central hole ($\varnothing 5\text{cm}$) for the passage of beam



SciFi2

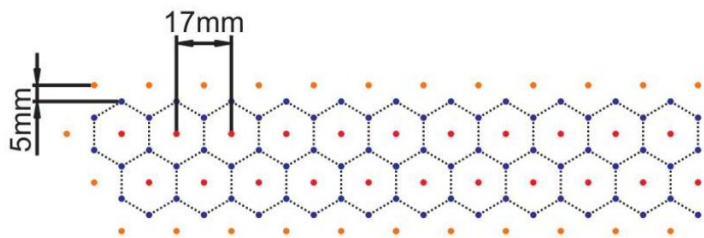
Scintillation fiber detector (66cmx51cm)
640 total channels
2 double layers x/y (352 and 288 rot. 90°)
Each single layer consists of two fiber arrays
(2.0mm track length for crossing particles)
Read-out 16 channel PM
Central hole ($\varnothing 4\text{cm}$) for the passage of beam



FORWARD SPECTROMETER: AFTER DIPOLE

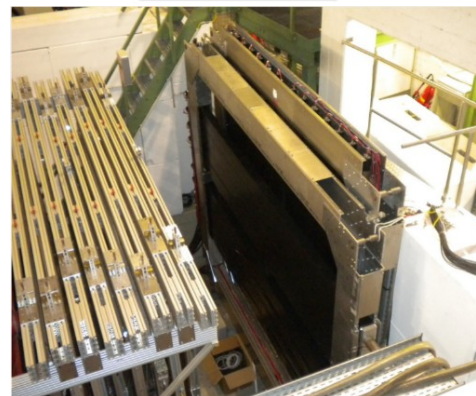
DRIFT CHAMBERS

Two sets of 4 double layers
X(vert.), Y(90°), U(+9°), V(-9°)
Sensitive area 1.2 x 2.4 m²
X = horizontal
Y = vertical
U = 99° w.r.t. X
V = 81° w.r.t. X
Hexagonally shaped drift cells (inner radius 8.5mm)
Distance from target = 3.8 m ÷ 4.5 m
Gas mixture: 70% Ar, 30% Co₂
Central insensitivity spot (5x5cm²)

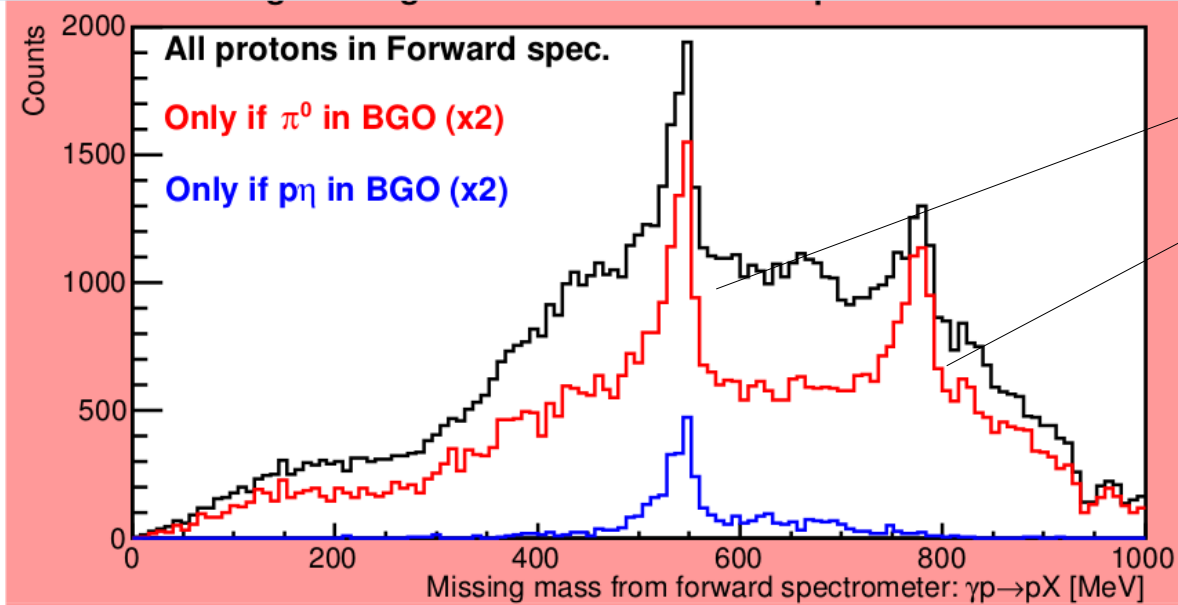


TOF WALLS

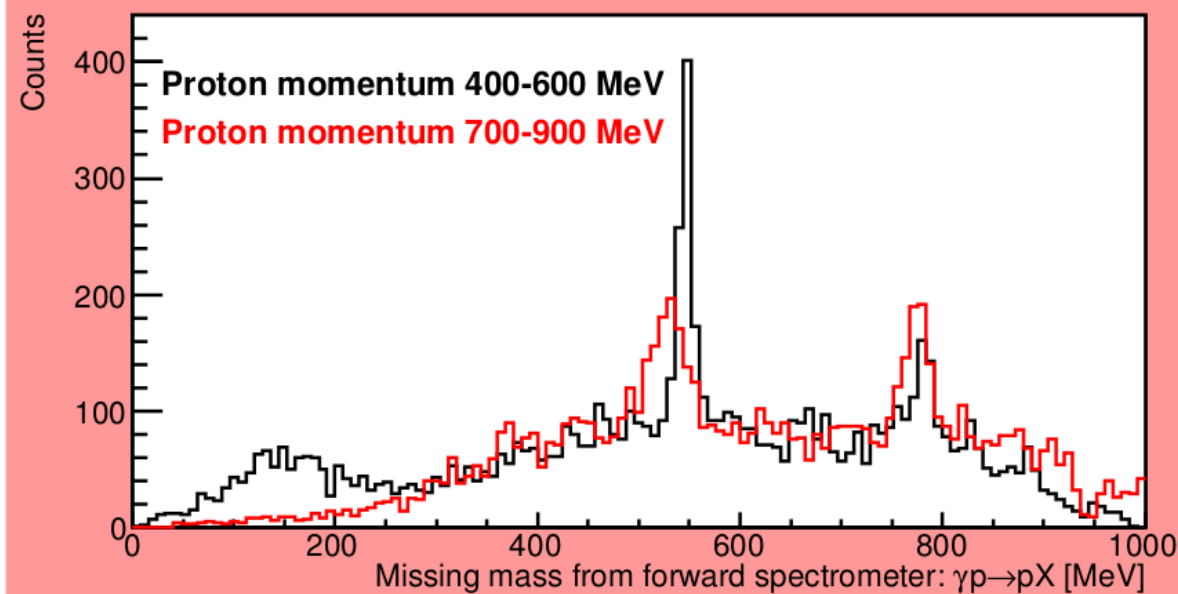
- 2 walls
- 14 bars vert., 8 bars hor.
- Scintillator dimensions:
 - 3400mm x 210mm x 60mm (horizontal bars)
 - 2700mm x 200mm x 45mm (vertical bars)
- Time resolution ~500ps
- Upgrade using former GRAAL ToF detectors (time resolution ~200ps) **JUNE 2014**



Missing Mass from Protons Detected in the Forward Spectrometer



$m_\eta \quad \eta \rightarrow 3\pi^0, \pi^+\pi^-\pi^0$
 $m_\omega \quad \omega \rightarrow \pi^+\pi^-\pi^0$



N.B. $p_{\text{proton}} > 400 \text{ MeV}/c$ in order to suppress π^0 photoproduction

FLUX MONITORS

Two flux monitors:

GIM (Gamma Intensity Monitor): efficiency close to 100%

Lead Glass

Uses the Cerenkov effect to separate charged particles from the e.m. showers generated by photons

One single lead block

2" PM



FLUMO (Flux Monitor)

Three scintillators + a Copper foil between the first and second scintillators

Low intensity runs to extract the efficiency of the FluMo

